



Benthic Ostracods as Pollution Indicator: A Case Study from Sharm Obhur, Red Sea Coast, Saudi Arabia

Mohammed H. Aljahdali¹ · Ramadan M. El-Kahawy² · Mohamed Elhag³ · Bandar A. Al-Mur⁴ · Andrew N. Quicksall⁵ · Faisal Alsaq⁶ · Ibrahim M. Ghandour^{1,7}

Received: 23 January 2024 / Revised: 6 July 2024 / Accepted: 28 August 2024
© King Abdulaziz University and Springer Nature Switzerland AG 2024

Abstract

The Red Sea has been consistently exposed to pollution from industrial waste, and ship activities, raising apprehensions about the potential ecological consequences for its marine ecosystems. Benthic ostracods, small crustaceans inhabiting surface sediment of shallow marine environments that are highly sensitive to environmental changes, were utilized in this study due to their usefulness as bioindicators. Thus, 47 sediment samples collected from Sharm Obhur, northern Jeddah, Saudi Arabia have been examined to assess the repercussion of environmental stresses on benthic ostracods. Spatial distribution patterns of heavy metals and organic pollutant exhibit significantly high concentrations around stations anthropogenically influenced at the sharm head and decline toward the Red Sea entrance. Moreover, these stations rendered low living ostracods percentage suggesting deterioration of their environment. Statistically, redundancy analysis categorized stations and benthic ostracods communities as well as environmental factors into two ecological biotopes. Biotope I comprises stations from the sharm head (i.e., O11, and O16) influenced by elevated heavy metals, and organic pollutants contents. High ostracod percentages of the tolerant-living *Hemicytheridea paiki* and *Alocopocythere reticulata* dominate these stations, while species diversity is low. Biotope II consists of stations near the Red Sea entrance (i.e., O47, and O44), and is populated by *Loxocorniculum ghardaqensis*, *Cyprideis torosa*, *Moosella striata*, and *Xestoleberis* spp. These taxa are accompanied by three controlling factors, CaCO₃%, water depth, and sand%. The study revealed an environmental system already expressing symptoms of anthropogenic degradation, emphasizing urgent need for prioritized recovery. Such information is crucial for effective management and conservation strategies in the Sharm Obhur ecosystem.

Keywords Benthic ostracoda · Heavy metals · PAHs and TPH · Sharm Obhur · Saudi Arabia

✉ Ramadan M. El-Kahawy
relkahawy@cu.edu.eg

Mohammed H. Aljahdali
maljahdli@kau.edu.sa

Mohamed Elhag
melhag@kau.edu.sa

Bandar A. Al-Mur
balmur@kau.edu.sa

Andrew N. Quicksall
aquicksall@smu.edu

Faisal Alsaq
falsaaq@kau.edu.sa

Ibrahim M. Ghandour
ighandour@kau.edu.sa;
ibrahim.ghandour@science.tanta.edu.eg

¹ Department of Marine Geology, Faculty of Marine Sciences, King Abdulaziz University, Jeddah 21589, Saudi Arabia

² Geology Department, Faculty of Science, Cairo University, Cairo 12613, Egypt

³ Department of Water Resources, Faculty of Environmental Sciences, King Abdulaziz University, Jeddah 21589, Saudi Arabia

⁴ Department of Environment, Faculty of Environmental Sciences, King Abdulaziz University, Jeddah 21589, Saudi Arabia

⁵ Department of Civil and Environmental Engineering, Southern Methodist University, Dallas, TX, USA

⁶ Department of Hydrographic Surveying Faculty of Maritimes Studies, King Abdulaziz University, P.O. Box 80401, Jeddah, Saudi Arabia

⁷ Department of Geology, Faculty of Science, Tanta University, Tanta 31527, Egypt

Abbreviations

A.r	<i>Alocopocythere reticulata</i>
H.p	<i>Hemicytheridea paiki</i>
M.s	<i>Miocyprideis spinulosa</i>
L.o	<i>Loxococoncha ornatovalvae</i>
L.e	<i>Lankacythere elaborata</i>
L.a	<i>Leptocythere arenicola</i>
C.p	<i>Cytherella punctata</i>
R.d	<i>Ruggieria danielopoli</i>
M.st	<i>Moosella striata</i>
L.gh	<i>Loxocorniculum ghardaqensis</i>
J.b	<i>Jugosocythereis borcheri</i>
T.g	<i>Tanella gracilis</i>
C.t	<i>Cyprideis torosa</i>
X.r	<i>Xestoleberis rotunda</i>
X.ro	<i>Xestoleberis rhomboidea</i>
P.f	<i>Paranesidea fracticorallicola</i>
P.s	<i>Pontoparta salina</i>
C.a	<i>Callistocythere arcuata</i>
L.g	<i>Loxococoncha gurneyi</i> . Dead: The dead ostracod%
Liv.	The living ostracod%
Div.	The species diversity

1 Introduction

The quality of shallow marine ecosystems in urban coastal regions is often significantly diminished due to the impact of human activities such as domestic and industrial waste discharge, aquaculture, and tourism (Lu et al. 2018). Coastal and nearshore marine areas, such as the Red Sea, are vulnerable to pollution from contaminants resulting from human activities (Monier et al. 2023). These contaminants have the potential to induce substantial disturbances across multiple trophic levels within marine ecosystems (Tuuri and Leterme 2023). Consequently, there has been a burgeoning interest in employing bioindicators to assess the ramifications of anthropogenic activities on these environments spanning the last few decades.

Bioindicators have gained global attention for monitoring the quality of an ecosystem (Parmar et al. 2016). While water quality analysis is a widely utilized method for monitoring pollution, it may not always detect all pollutants or identify the early stages of negative biological impacts (Ghetti 1980; Parmar et al. 2016). By analyzing the composition, abundance, and structure of bioindicator populations, valuable insights can be obtained on the prevailed environmental conditions (Rinderhagen et al. 2000). Benthic ostracods, a type of crustacea with a calcified carapace, are well-documented and inhabit a wide range of aquatic environments, comprising marine, brackish, and freshwater habitats (Mohammed and Keyser 2012). They can be

regarded as a part of the microfauna that have been utilized as bioindicators for episodically stressed environments (Anadon et al. 2002; Boomer and Eisenhauer 2002). Ostracods have been employed to assess environmental changes caused by natural processes such as changes in salinity, pH, and temperature, as well as anthropogenic impacts like sewage discharge, agricultural and industrial activities, urban effluent waters, and heavy metals dispersions (Ruiz et al. 1997; Bodergat et al. 1998; Egar 1999; El-Kahawy et al. 2021). Furthermore, benthic ostracods assemblage of low salinity levels such as brackish waters display morphological nodes and/or punctate forms (Külköylüoğlu et al. 2023). On the other hand, anthropogenic impacts can cause benthic ostracods to relocate from polluted to unpolluted locations (Samir 2000).

Heavy metals, known for their potentially toxic characteristics, pose a significant threat to aquatic life, particularly biota (e.g., Kumar et al. 2019). Various types of pollutants, including heavy metals, toxic organic components, and crude oil, can impact the abundance and distribution of benthic ostracods (Sundelin and Elmgren 1991; Samir 2000; El-Kahawy et al. 2021). High levels of heavy metals in sediments negatively affect benthic ostracods, leading to a decrease in species diversity as well as numbers of individuals, and changes in the composition of the ostracod community (Samir 2000; Ruiz et al. 2005, 2013; Cibic et al. 2012; El-Kahawy et al. 2021). However, it has been shown that marine environments may include highly diversified ostracod assemblages with exceptionally elevated levels of heavy metals (Aiello et al. 2020, 2021).

Among the anthropogenic organic pollutants, polycyclic aromatic hydrocarbons (PAHs) and total petroleum hydrocarbon (TPH) are of significant environmental concern due to their potential toxicity and carcinogenicity to both ecosystem and human health (Scott et al. 2012; Liang et al. 2020). The accumulation of PAHs and TPH in sediments is influenced by sediment composition, particularly the content of organic matter (Goswami et al. 2016). PAHs have the potential to enter the food chain when they are transferred from polluted sediments to the surrounding water or to bottom-dwelling organisms that consume organic matter (Eek et al. 2008). This bioaccumulation through the food chain may increase the risk of cancer and other adverse human health effects (Liu et al. 2016). Studies have shown that PAHs hinders bacterial growth and leads to reduced cell production (Johnsen et al. 2002); further, PAHs and their epoxides exhibit significant toxicity, carcinogenicity, and mutagenicity for microorganisms (Abdel-Shafy and Mansour 2016). The Red Sea, particularly Sharm Obhur, has been subjected to anthropogenic and natural sources of petroleum hydrocarbons (Rushdi et al. 2019; Bantan et al. 2024). Anthropogenic inputs from offshore oil fields,

petrochemical plants, liquid refineries, sewage effluents, and shipping operations pose significant threats to the broad Red Sea ecosystem (Mandura 1997; El Nemr et al. 2014). Sewage discharge is threatening marine biota due to contaminant composition of the effluent. The Red Sea is suffering from oil ships, cargo vessels, and private yacht sewage as well as domestic sewage (Hees 1977; Badr et al. 2009). Benthic ostracods have shown a significant negative correlation with organic contaminants ‘petroleum hydrocarbon’ in terms of species numbers and faunal abundance (Carman et al. 2000), highlighting their sensitivity as bioindicators, particularly ostracods and copepods (Peterson et al. 1996). Consequently, the presence of petroleum hydrocarbon contaminants is known to impact the composition of the benthic community (Carman and Todaro 1996).

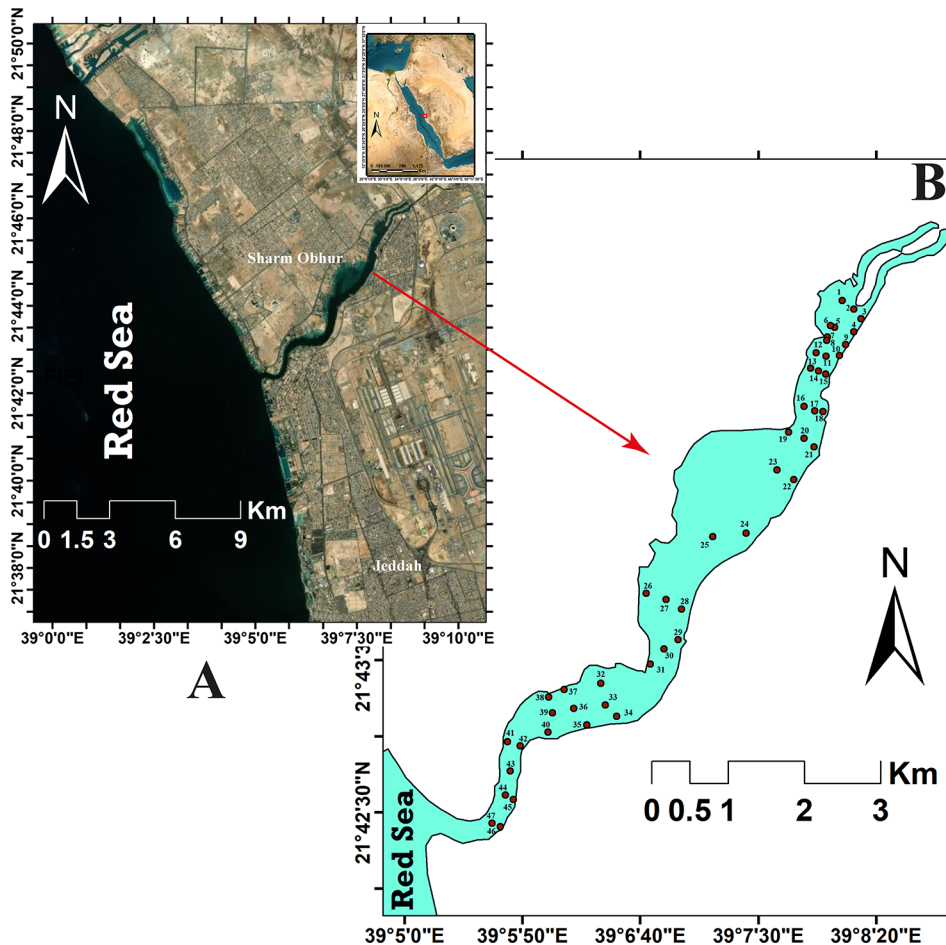
To the best of our knowledge, studies focusing on the utilization of ostracods as bioindicators for pollution in Sharm Obhur are currently lacking. While there have been numerous investigations into the marine life and ecology of the area, none have specifically addressed the potential of ostracods as a biomonitoring tool for ecosystem threat. Considering the sensitivity of ostracods to environmental changes and their proven efficacy as pollution indicators in

other marine ecosystems, further exploration in this domain could yield valuable insights into the marine environment’s condition in Sharm Obhur. Consequently, this study has multiple objectives, including: (1) evaluating the levels and sources of pollution in the marine environment of Sharm Obhur, encompassing heavy metals, and organic pollutants, (2) identifying the areas most impacted by pollution and assessing the potential consequences on the health of the marine ecosystem, (3) investigating the viability of ostracods as a biomonitoring tool in the Red Sea region.

2 Study Area Description

Sharm Obhur, situated ~35 km north of Jeddah City, Saudi Arabia, is a coastal coralline limestone lagoon naturally cut in the Red Sea region (Fig. 1). The sharm is an attractive and over-crowded area for recreational activities and marine cruises. It is a semi-enclosed system occupied by several shipyards, sewage discharges from restaurants, and marinas as well as touristic villages. During the field survey, the bottom surface of the sharm was occupied by dumped litters such as plastics and cans (Basaham et al. 2006),

Fig. 1 A. Google Earth map shows the location of the study area, B. Sampling stations spatially mapped along Sharm Obhur



which in turn may influence the marine biota negatively. Furthermore, huge number of ships docking and oil changes for motors engine is also observed, hence may impact on marine life if effluent into water. On the other hand, Sharm Obhur is suffering from uncontrolled coastal urbanization and over development human activities (Basham et al. 2006). They reported that the surface area of Sharm Obhur declined by 800,000 m² due to land reclamation, urbanization, and construction of recreational and tourism amenities along its beaches.

Sharm Obhur ecosystem is characterized by its diversified marine habitat, which includes coral reefs, seagrasses, and a wide range of marine organisms such as fish, sharks, and sea turtles. The coral reefs community of Sharm Obhur was investigated by Wilson et al. (2017). They recognized a fringing reef structure that houses a wide variety of coral genera, including *Acropora*, *Porites*, and *Montipora*. The study also highlighted the prevalence of seagrass dominated by *Halodule uninervis* and *Halophila ovalis*, which play a crucial role as micro-habitats for a wide range of marine organisms. The water depth of the Sharm Obhur stations exhibits a range from 1 m to 30 m (Table 1), where it is connected to the Red Sea through a narrow inlet measuring approximately 250 m in width (Rasul 2015). The coastal sectors of the lagoon are made up of Quaternary sandy beaches and rocky cliffs. Surface water temperature measurements ranged between 24.4 °C and 32.2 °C, while water salinity fluctuates between 39.11‰ and 40.14‰ during winter and summer, respectively (Basaham and El-Shater 1994; AlSaa-fani et al. 2017). Sharm Obhur experiences mixed semidiurnal tides characterized by a relatively small tidal range of approximately 0.3 m (Ahmad and Sultan 1993; Shamji and Vineesh 2017). The wind and wave patterns in Sharm Obhur are influenced by the local and regional meteorological conditions, as well as the topography of the area. According to Al-Farawati et al. (2019), the Red Sea undergoes a predominant northerly wind, known as the Shamal, which blows from the north and northwest during the winter months (October to April) and can reach speeds of up to 20 knots. During the summer months (May to September), the winds are typically lighter and more variable, with occasional southerly winds blowing from the south and southeast.

3 Materials and Methods

3.1 Sampling Procedure

In November 2021, a northeast-southwest transect consisting of 47 sites was sampled (Fig. 1). The sediment samples (uppermost 1–2 cm) were collected using a Van Veen grab sampler (15×15×30 cm) deployed from a small fishing

boat. The sediment sample of the coastal station (≤ 3 m water depth) were collected, by divers, via hand-held plastic coring tube whose inner diameter is 8 cm. From each site, triplicates were acquired allowing reliable and informativeness dataset of the benthic ostracod assemblage for biomonitoring work (Bouchet et al. 2012). The sediment replicates of stations deeper than 3 m were acquired using grab sampler, while the coastal stations (≤ 3 m) were captured by different deployments from three nearby places at the same site. The water depth was measured using a UWTEC Eco-sounder, while salinity, temperature, and pH were measured in situ using a YSI 556 MPS instrument (Table 1). The coordinates of each site were determined using a hand-held Garmin II GPS device.

The collected samples were placed in clean, labelled polyethylene bags, stored in a freezing icebox, and transported to the laboratory. In the lab, samples were dried at room temperature, homogenized, and divided into aliquots for textural, chemical, loss on ignition (LOI), and micro-paleontological analyses, following the FOBIMO protocol (Schönfeld et al. 2012).

To distinguish living ostracods from dead ones, a staining process using a rose Bengal solution was employed as well as a careful examination of soft tissues was conducted during the identification process. The rose Bengal solution, prepared at a concentration of 2 g/L in 95% ethanol (Schönfeld et al. 2012), selectively stained the appendages of living ostracods in the sediment sample. Using a Leica stereomicroscope (60X magnification), the stained shells were examined, counted, and the presence or absence of dense, vividly rose-stained protoplasm within the shells indicated a living ostracod was noted (Walton 1952; Barras et al. 2014).

3.2 Laboratory Analyses

20 g of each sediment sample were utilized for the purpose of conducting grain size analysis. The analysis followed the method proposed by Folk and Ward (1957) and employed the standard sieve and sedimentation technique for granulometric analysis.

A weight-loss method based on acid treatment was used to assess the total carbonate content, as reported by Gross (1971). The dried sediments were treated with a dilute hydrochloric acid solution (2.5 N), and the residue was collected on a 0.45 µm filter. After drying the filter, the observed weight loss was converted into a percentage to represent the carbonate content.

The determination of organic matter in the sediment was carried out using a sequential weight loss method at a temperature of 550 °C, following the procedure outlined by Dean (1974).

Table 1 The stations latitudes and longitudes, environmental factors (pH, Temperature, water depth, Salinity, total organic matter (TOM%), and CaCO₃%), and sediment grain size% (Gravel, Sand, and Mud) of Sharm Obhur stations

Station	Latitude (°N)	Longitude (°E)	pH	Temperature (°C)	Water depth (m)	Salinity ‰	Total organic matter (%)	CaCO ₃ (%)	Gravel %	Sand %	Mud %
O1	21°45.839	039°08.138	8.08	31.11	1	39.95	6.75	8.26	1.09	61.78	37.13
O2	21°45.791	039°08.179	8.02	31.16	5	39.85	5.41	6.42	0.23	64.02	35.75
O3	21°45.746	039°08.233	8.11	31.24	5	39.88	6.9	23.28	4.2	52.03	43.77
O4	21°45.657	039°08.158	8.09	31.11	5	39.85	7.01	8.22	0.22	62.01	37.77
O5	21°45.664	039°08.092	8.19	31.15	6	39.82	5.65	6.07	0.12	55.3	44.58
O6	21°45.696	039°08.042	8.15	31.15	3	39.81	5.61	56.79	27.24	47.07	25.69
O7	21°45.620	039°08.019	8.12	31.14	7	39.84	6.67	39.46	0.29	63.64	36.07
O8	21°45.588	039°08.005	8.14	31.14	7	39.78	5.83	7.8	0.17	54.45	45.38
O9	21°45.576	039°08.119	8.15	31.12	5	39.8	5.51	47.48	7.33	74.13	18.54
O10	21°45.491	039°08.065	8.11	31.12	7	39.76	3.54	45.49	9.29	79.1	11.61
O11	21°45.498	039°08.007	8.12	31.1	9	39.74	7.56	10.82	0.1	57.03	42.87
O12	21°45.521	039°07.949	8.11	31.1	8	39.76	6.55	74.64	8.4	66.24	25.36
O13	21°45.333	039°07.873	8.13	31	12	39.73	7.33	19.3	0.06	25.64	74.3
O14	21°45.324	039°07.915	8.14	31	11	39.75	8.3	13.22	0.1	19.89	80.01
O15	21°45.297	039°07.944	8.14	30.95	10	39.72	6.15	10.78	0.17	30.53	69.3
O16	21°45.094	039°07.915	8.08	30.95	11	39.68	8.84	17.99	0	14.31	85.69
O17	21°45.095	039°07.862	8.16	30.85	12	39.65	5.91	19.46	0	14.74	85.26
O18	21°45.118	039°07.803	8.12	30.85	7.5	39.63	4.4	84.23	1.26	88.7	10.04
O19	21°44.956	039°07.716	8.2	30.85	2	39.62	4.05	78.73	8.23	64.64	27.13
O20	21°44.924	039°07.796	8.19	30.8	12	39.64	8.76	31.38	0	14	86
O21	21°44.872	039°07.856	8.16	30.8	18	39.61	6.64	42.74	1.01	36.63	62.36
O22	21°44.659	039°07.683	8.15	30.8	17	39.6	8.51	27.94	0	10.84	89.16
O23	21°44.692	039°07.619	8.2	30.76	15	39.58	5.24	77.02	7.35	69.49	23.16
O24	21°44.318	039°07.385	8.14	30.76	17	39.62	10.04	40.08	2.67	7.82	89.51
O25	21°44.342	039°07.243	8.17	30.72	16	39.56	5.78	80.69	0	71.64	28.36
O26	21°43.955	039°06.750	8.23	30.65	1.5	39.55	3.85	91.67	32.5	63.46	4.04
O27	21°43.915	039°06.875	8.21	30.6	22	39.53	12.76	47.92	0.1	7.19	92.71
O28	21°43.865	039°06.961	8.18	30.65	18	39.55	11.02	41.08	0	3.32	96.68
O29	21°43.638	039°06.932	8.15	30.65	13	39.51	9.92	29.63	0	14.26	85.74
O30	21°43.611	039°06.86723	8.18	30.62	23	39.54	10.25	43.82	0	8.07	91.93
O31	21°43.537	039°06.778	8.19	30.62	3	39.5	2.63	88.89	31.26	64.66	4.08
O32	21°43.298	039°06.393	8.2	30.55	5	39.45	3.82	83.45	4.42	66.74	28.84
O33	21°43.208	039°06.428	8.21	30.6	25	39.45	9.29	58.39	0	6.81	93.19
O34	21°43.133	039°06.487	8.17	30.55	25	39.47	9.51	53.07	0.19	27.59	72.22
O35	21°43.057	039°06.304	8.2	30.52	3	39.45	6.14	80.18	0.7	68.16	31.14
O36	21°43.189	039°06.219	8.15	30.47	24	39.45	11.61	50.64	0	6.44	93.56
O37	21°43.292	039°06.116	8.16	30.52	3	39.4	3.13	89.79	20.78	74.29	4.93
O38	21°43.228	039°06.030	8.23	30.5	3	39.35	3.9	90.1	37.73	58.27	4
O39	21°43.166	039°06.075	8.2	30.45	27	39.35	8.7	50.94	0	3.87	96.13
O40	21°43.075	039°06.037	8.21	30.5	4	39.3	4.18	90.71	1.23	92.94	5.83
O41	21°42.945	039°05.735	8.18	30.4	27	39.25	9.02	64.49	0.89	36.35	62.76
O42	21°42.934	039°05.796	8.21	30.38	23	39.25	5.04	91.42	18.19	73.68	8.13
O43	21°42.789	039°05.750	8.23	30.4	25	39.21	11.74	55.96	0	5.23	94.77
O44	21°42.606	039°05.702	8.2	30.35	25	39.16	5.26	75.24	1.72	52.98	45.3
O45	21°42.581	039°05.751	8.21	30.38	28	39.16	5.24	75.96	6.53	56.14	37.33
O46	21°42.417	039°05.635	8.19	30.3	30	39.15	7.87	60.1	0.31	50.75	48.94
O47	21°42.438	039°05.588	8.2	30.25	3	39.15	3.49	88.89	10.82	79.93	9.25

3.2.1 Ostracod Analysis

20 g of each sediment sample were sieved through a 500 μm , 300 μm , 250 μm , 125 μm , and 63 μm mesh sieves. The sieved samples were subsequently placed into an oven for drying at 50 $^{\circ}\text{C}$ for 2 h, to facilitate the isolation of the ostracod individuals. The benthic ostracods were picked using a 000-sable hairbrush under a binocular stereomicroscope (60X). The collected specimens, including both individual valves and connected carapaces, were quantified. In the counting process, each individual valve was considered as 0.5 specimen, while each complete carapace was treated as a single specimen. The identification process was performed on the ostracod taxa $> 125 \mu\text{m}$. The ostracod individuals were identified using internal and external valve characteristics, as described in taxonomic literature Moore (1961); Hartmann (1964), Bonaduce et al. (1976); Bonaduce et al. (1980); Bonaduce et al. (1983), Mostafawi (2003), Helal and Abd El Wahab (2004); Martens and Horne (2009), Mohammed and Keyser (2012), El-Kahawy et al. (2021), Keyser and Mohammed (2021). The identified ostracod

taxa were photographed using scanning electron microscope (JSM 6063LA) at the Egyptian Mineral Resources Authority (EMRA) and illustrated in Fig. 2. The incident beam energy focused on the specimen surface (coated by thin gold layer) is 20 keV.

3.2.2 Heavy Metals, TPH, and PAH in Sediments

The heavy metals such as Copper (Cu), Chromium (Cr), Nickel (Ni), Cobalt (Co), Zinc (Zn), Lead (Pb), Arsenic (As), and Vanadium (V) in the sediment samples were analyzed in Acme labs (Vancouver, Canada) via inductively coupled plasma-mass spectrometry (ICP-MS). Samples were processed by grinding to yield particles smaller than 0.25 mm. To leach the sulphides, and some oxides, 0.5 g of each sample followed a careful partial digestion using aqua regia solution, involving 0.6 ml concentrated Nitric acid (HNO_3), 1.8 ml concentrated Hydrochloric acid (HCl), and 0.5 ml Water (H_2O) is performed. The digestion was carried out for a duration of 2 h at 95 $^{\circ}\text{C}$. The sample residue was dissolved by heating with 5 ml of a 1:1 HNO_3 solution.

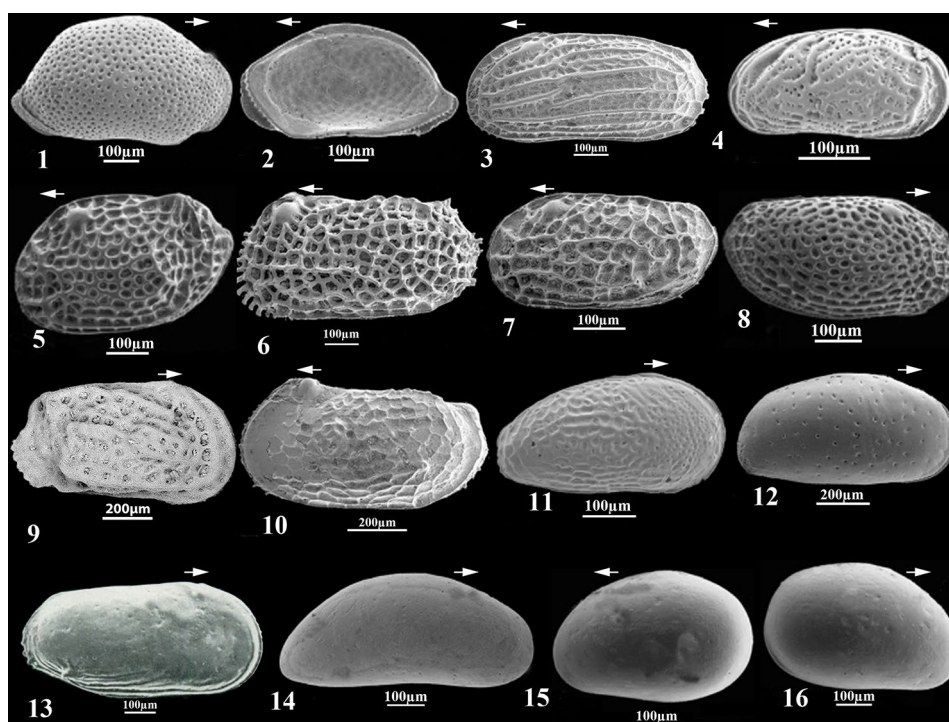


Fig. 2 Photomicrographs for the most abundant benthic ostracods species of Sharm Obhur site, the white arrow oriented towards anterior direction, **1–2.** *Paranesisidea fracricorallicola* Maddocks, 1969, **1-** external view, **2-** internal view, right valve, sample O44, **3.** *Moosella striata* Hartmann 1964; external view, left valve, sample O21, **4.** *Leptocythere arenicola* (Hartmann 1964), external view, left valve, sample O47, **5.** *Loxocorniculum ghardaqensis* Hartmann 1964; external view, left valve, sample O41, **6.** *Lankacythere elaborata* Whatley and Zhao, 1988, external view, left valve, sample O26, **7.** *Loxoconcha ornativalvae* Hartmann 1964; external view, left valve, sample O40, **8.** *Loxoconcha gurneyi* Bate and Gurney, 1981, external view, right

valve, sample O39, **9.** *Jugosocythereis borchersi* (Hartmann 1964), external view, right valve, sample O36, **10.** *Alocopocythere reticulata* (Hartmann 1964), external view, left valve, sample O23, **11.** *Hemicythereidea paiki* Jain, 1978, external view, right valve, sample O19, **12.** *Cyprideis torosa* (Jones 1850), external view, right valve, sample O19, **13.** *Ruggieria danielopoli* Hartmann 1964; external view, right valve, sample O21, **14.** *Pontoparta salina* Harding, 1954, external view, right valve, sample O17, **15.** *Xestoleberis rotunda* Hartmann 1964; external view, left valve, sample O44, **16.** *Xestoleberis rhomboidea* Hartmann 1964; external view, right valve, sample O43

The sample was cooled after digestion and acid elimination, diluted to 10 ml with de-ionized water, and homogenized. Subsequently, 5 ml of a 4 ppm Indium standard solution was added. The resulting mixture, consisting of the sample and reference solutions, was then introduced into the ICP-MS instrument using a peristaltic pump set at a flow rate of 0.18. The samples were analyzed using a Perkin-Elmer Sciex Elan 5000 ICP-MS for the heavy metal suite. Before each measurement, the nebulizer and spray chambers were subjected to a thorough washing procedure. This involved introducing a solution into the system for a duration of 3 min., with a 0.5 revolutions per minute (rpm). Following that, an additional 30-second washing step was conducted at 0.18 rpm. These meticulous cleaning steps ensured the removal of any potential contaminants or residues, thereby maintaining the integrity and accuracy of subsequent measurements.

The hydrocarbon concentrations measurements, total petroleum hydrocarbons (TPH) and polycyclic aromatic hydrocarbons (PAHs), were determined using the USEPA 3540 C method for extracting and cleaning sediments. Briefly, approximately 20 g of each sediment samples were cleaned and labelled in an extraction thimble. Sediment samples were extracted using a Soxhlet apparatus with a 400 ml of an isotropic mixture of dichloromethane and methanol (93:7 v/v) for 48 h. Prior to extraction, an internal standard (1-eicosene) was included in the sediment to assist with quantification and to enhance the elucidation of saturated hydrocarbons. Activated copper turnings were added to clean the extract and remove elemental sulphur. The extracts were dried by adding anhydrous sodium sulfate. The concentrations of total petroleum hydrocarbons (TPH) were quantified by UV-spectrofluorometer (Shimadzu RF-5000) measurement of the compound fluorescence intensity (excitation at 310 nm and emission at 360 nm). Quantification and standardization were conducted on light Arabian oil.

Clean up and isolation of hydrocarbon fractions were carried out by column chromatography with activated silica gel. Elution with hexane-dichloromethane (50:50 v/v) yielded the aromatic hydrocarbon fraction (Jeffrey and Saitas 2001). Gas chromatography-flame ionization detection (GC-FID) was used for quantitative and qualitative analysis of PAHs. The polycyclic aromatic hydrocarbons (PAHs) were determined by measuring their fluorescence intensity (excitation 310 nm and emission at 360 nm) using UV-spectrofluorometer (Shimadzu RF-5000). Standardization and quantification were performed using chrysene substance (Law and Whinnet 1992).

3.3 Statistical Analysis

The relative abundances of ostracod assemblages were statistically processed, focusing on the living taxa that had an

occurrence of more than 2%. Using XLSTAT software, a hierarchical cluster analysis was generated to visually indicate the correlation coefficient values in a matrix of varying degrees. The dendrogram of the samples (Q-mode) and species (R-mode) was illustrated based on their similarity index. The dataset was transformed and normalized in a reduced model and centred standardization type. The clustering method was created using non-specific filtering feature which screens poor variation among individuals, thereby improving the readability of the dendrogram; 0.25 interquartile range was used for filtering the dataset. The agglomeration of the dendrogram was performed via Euclidean dissimilarity measurement with noisy observation < 0.5 .

Redundancy analysis (RDA), specifically multivariate ordination method, was applied to explore the relationships between environmental (response) and biological (explanatory) variables. This method reveals linear combinations of data that explain the variation in environmental variables, while accounting for the effects of other variables. A principal procedure involved in conducting RDA analysis involved performing Pearson correlation analysis to identify which oceanographic variable had a significant influence on the ostracod distribution pattern. Only the variables; CaCO_3 , and water depth showed significant strong positive coefficients due to their high variations, thereby included in the RDA analysis. On the other hand, the salinity, pH, and temperature exhibited weak coefficients, hence were omitted from the analysis due to their low variations among different stations. The RDA technique was chosen due to the response data having a gradient 1.4 standard deviations units long, making the linear method the recommended strategy (Šmilauer and Lepš 2014). To assess the significance of the explanatory variables individually, a permutation test with 499 iterations was applied. The dataset of the response variables was square root transformed, centered, and standardized. These calculations were done using CANOCO software, version 5.15.

The comprised association among species richness and species abundance is delineated through diversity indices. The calculation of diversity indices was accomplished using the Paleontological Statistics software V. 4.08 (Hammer et al. 2009).

4 Results

4.1 Oceanographic Parameters

The water temperature, salinity, and pH measurements recorded in November 2021 at Sharm Obhur are presented in Table 1. The mean water temperature measured at Sharm Obhur was 30.76 °C. Concurrently, the average

salinity of the water was recorded at $\sim 39.6\%$, and the pH level averaged at ~ 8.2 . At O47, near the Sharm Obhur head, the temperature dropped to a low of $30.25\text{ }^{\circ}\text{C}$, meanwhile, O3, located towards the head of the sharm, experienced the highest temperature of $31.24\text{ }^{\circ}\text{C}$. The data in Table 1 clearly indicates a slight decrease in water temperature towards the southwest. The salinity values varied among the sampling stations, with O46 and O47 (sharm mouth) recording the lowest values of 39.15% , whereas O1 (sharm head) recording the highest value of 39.95% . In addition, the pH values at the sampled stations ranged from 8.02 at O2 to 8.23 at O38 and O43 (Table 1).

4.2 Environmental Variables

4.2.1 Bottom Sediments Characteristics

The sediment grain size analysis conducted in the study area revealed that the proportion of the gravel fraction ($> 2\text{ mm}$) is low, with a mean value of 5.2% (Fig. 3A). Furthermore, at several stations, it is not detected as shown in Fig. 3A. However, at O38, the gravel fraction is found to be the highest ($> 37\%$), with the main contribution coming from biogenic remains of corals and molluscs.

In contrast, the sand fraction ($2\text{--}0.063\text{ mm}$) is also relatively high in the sediment samples, encompassing an average of 45% of the total sediments (Fig. 3B). This fraction is found to be predominant at all of the studied stations, with a maximum of up to 96% at certain stations (Fig. 3B). Biogenic remnants of benthic foraminifera, corals, small molluscs, and calcareous algae are the primary contributors to the sand fraction.

The mud fraction ($< 0.063\text{ mm}$) is the most prevalent sediment grain size, with an average value of 49.5% (Fig. 3C). However, it reached the highest values in sheltered stations O28 (96.7%), while the lowest value is observed beyond O38 (4%) (Fig. 3C).

4.2.2 Total Organic Matter (TOM) and Carbonate Content

The total organic matter analysis exhibited a high TOM value in the southwestern direction (sharm entrance) and certain stations in the northeastern sector (sharm head; O16), with a mean value of 6.8% (Fig. 3D). The highest value of organic matter ($\sim 13\%$) is observed at O27, while the lowest value is recorded beyond O32 (3.82%).

The CaCO_3 content displayed a consistent increasing trend in the vicinity of the sharm entrance stations, with a mean value of 50.7% . Additionally, the highest CaCO_3 content is quantified at O26 and O42 ($\sim 91.5\%$), whereas the lowest values are detected at the sharm head, involving O1, O2, O4, O5, and O8 (Table 2).

4.3 Heavy Metals and Hydrocarbons (TPH and PAH) Concentrations

The sediment samples obtained from Sharm Obhur exhibited comparatively small levels of Cu, with an average concentration of $\sim 21\text{ }\mu\text{g/g}$. Conversely, a substantial rise in Cu concentration was observed in the samples of the sharm head, with values as high as $43\text{ }\mu\text{g/g}$ in the vicinity of station O1 (Fig. 4A). The average concentration of Cr is $\sim 45\text{ }\mu\text{g/g}$, while the highest value was obtained from stations O2 and O5 ($92\text{ }\mu\text{g/g}$) near the sharm head, and the lowest recorded value is from station O40 ($3\text{ }\mu\text{g/g}$) closer to the sharm entrance (Fig. 4B). The concentration of Ni is generally low across the studied stations, with an average value of $\sim 23.5\text{ }\mu\text{g/g}$ (Fig. 4C). The highest Ni concentrations were measured from O14 ($49.4\text{ }\mu\text{g/g}$), followed by O8 ($47.9\text{ }\mu\text{g/g}$) nearby the sharm head, whereas the lowest measured value was observed around station O40 ($0.7\text{ }\mu\text{g/g}$) toward the sharm entrance. The concentration of Co was relatively low, with a mean value of $\sim 8.5\text{ }\mu\text{g/g}$. The highest Co concentrations were observed near station O8 ($17.2\text{ }\mu\text{g/g}$), followed by O11 ($17\text{ }\mu\text{g/g}$), whereas the lowest concentrations were measured from stations O40 ($0.6\text{ }\mu\text{g/g}$), followed by O38 ($0.7\text{ }\mu\text{g/g}$) (Fig. 4D). The Zn concentration exhibits higher values at the sharm head, with an average of $41.5\text{ }\mu\text{g/g}$ (Fig. 5A). The station O14 rendered the highest Zn value ($76\text{ }\mu\text{g/g}$), whereas the lowest concentrations were detected beyond stations O38 and O31 ($5\text{ }\mu\text{g/g}$) (Fig. 5A). The overall Pb values are low, with an average of $\sim 5.2\text{ }\mu\text{g/g}$. The highest Pb values were observed near O36 ($8.6\text{ }\mu\text{g/g}$) followed by O43 ($8.4\text{ }\mu\text{g/g}$), whereas O31 has the lowest value recorded $1.1\text{ }\mu\text{g/g}$ (Fig. 5B). The average value of the As concentration is $\sim 7.1\text{ }\mu\text{g/g}$, with the highest concentrations observed around stations O13 and O21 ($12\text{ }\mu\text{g/g}$), while the lowest value was measured at O40 ($0.5\text{ }\mu\text{g/g}$) (Fig. 5C). The average V value is $\sim 61\text{ }\mu\text{g/g}$, with the highest concentrations observed at O1 ($130\text{ }\mu\text{g/g}$) followed by O2 ($128\text{ }\mu\text{g/g}$), and O5 ($127\text{ }\mu\text{g/g}$), whereas the lowest concentrations were measured at O40 and O38 ($4\text{ }\mu\text{g/g}$), followed by O26, & O42 ($4\text{ }\mu\text{g/g}$), and O37 ($7\text{ }\mu\text{g/g}$) (Fig. 5D).

The distribution patterns of TPH and PAHs in Sharm Obhur, as depicted in Fig. 6, exhibit a distinct classification between the sharm's entrance and head stations. The average concentrations of TPH and PAHs were found to be $\sim 35.5\text{ }\mu\text{g/g}$ and $\sim 10.1\text{ }\mu\text{g/g}$, respectively. The highest recorded TPH and PAHs values were observed toward the sharm head, specifically at O16 that has concentrations of $\sim 69\text{ }\mu\text{g/g}$ and $\sim 16\text{ }\mu\text{g/g}$, respectively (Fig. 6A and B). Conversely, the lowest concentrations were documented at the sharm entrance (O47) with values of $\sim 5.6\text{ }\mu\text{g/g}$, and $\sim 3.3\text{ }\mu\text{g/g}$, respectively. Notably, the sharm head exhibited the highest levels of TPHs concentrations in the vicinity

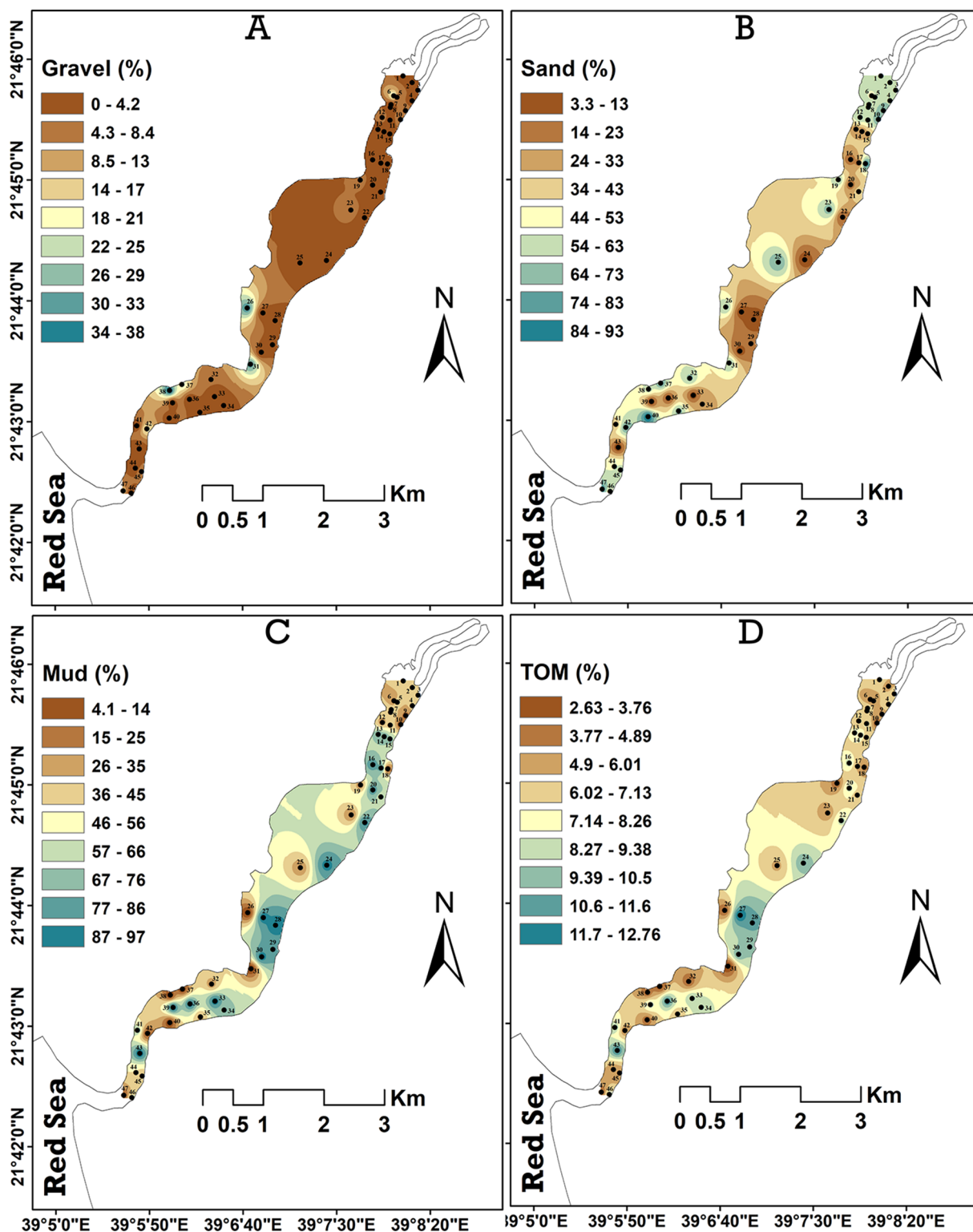


Fig. 3 Spatial bubble distribution maps for the granulometric analysis and total organic matter content in the Sharm Obhur site

of the following stations O16, followed by O8, O13, O11, O15, O1 and O14, respectively (Fig. 6). Additionally, the highest measured PAHs concentrations displayed the following order O16>O15>O11>O14>O5>O8>O2. On

the other hand, the lowest TPH and PAHs concentrations were observed at O47, followed by O42, O40, O38, O32, and O31 respectively (Fig. 6A and B).

Table 2 The measured heavy metals concentrations of the Sharm Obhur sediment samples as well as their total petroleum hydrocarbon (TPH), and polycyclic aromatic hydrocarbons (PAHs)

Station	TPH	PAH	V	Cr	Co	Ni	Cu	Zn	Pb	As
O1	67.74	13.61	130	87	14.6	39.1	43.2	72	5.8	9
O2	64.63	14.24	128	92	16.5	44.4	32.5	67	5.6	9
O3	45.5	11.1	96	63	12.2	31.2	26.3	52	5.2	9
O4	66.5	13.18	124	89	16.3	44.8	31.2	63	5.6	9
O5	67.42	14.56	127	92	16.9	46.2	33.3	68	5.8	9
O6	35.36	9.81	59	44	8.5	22.8	18.3	40	3.7	7
O7	44.71	12.3	79	62	11.3	30.7	23.4	51	5.6	10
O8	69.21	14.42	125	89	17.2	47.9	34.4	70	6.5	10
O9	33.21	9.95	66	39	8.2	19.4	17.3	57	6.9	9
O10	22.76	8.98	43	24	4.8	11.5	9.8	19	2.5	6
O11	68.31	15.78	119	91	17	47.1	34.7	72	6.6	10
O12	31.45	8.88	49	36	7.4	19.3	16.7	35	4.2	11
O13	68.44	12.91	102	78	15.1	43.5	35.7	69	7.5	12
O14	67.5	14.93	115	91	17	49.4	39	76	7.5	11
O15	68.1	15.87	116	89	16.4	45.6	34.3	71	7.4	10
O16	69.41	15.92	107	89	15.7	44.6	35.5	70	7.7	11
O17	66.33	12.15	109	84	16	46.6	37	73	7.7	11
O18	16.54	8.52	23	16	2.7	6.8	5.5	14	2	5
O19	18.56	8.63	24	20	3	7.4	6.1	14	1.9	3
O20	41.43	10.45	84	67	12.3	35.7	29	58	7	10
O21	40.21	10.22	78	58	10.9	31.5	27.2	54	7.1	12
O22	39.56	10.31	65	53	10.1	30.5	27.9	54	7.2	10
O23	18.67	8.54	24	17	3.4	9.1	9.6	19	3.1	6
O24	41.21	10.31	75	62	11.4	33.5	32.5	60	7.7	11
O25	16.87	8.43	19	12	2.5	6.4	6.8	14	2.7	5
O26	11.56	6.92	6	5	0.8	1.8	2.4	6	1.7	2
O27	40.1	10.24	64	50	9.7	29.2	26.5	52	7.2	10
O28	40.44	10.32	93	56	13.1	29.4	28.8	57	6.8	11
O29	39.66	10.21	93	54	12.1	27.4	27.8	54	5.8	6
O30	40.89	10.26	62	50	9.6	29.9	27.6	53	7.3	10
O31	10.42	6.92	8	5	0.9	1.7	2.2	5	1.1	2
O32	9.43	5.98	13	8	1.6	3.5	13.9	14	3.7	2
O33	29.51	9.33	45	37	6.5	19.6	19.8	39	6.2	7
O34	30.3	9.54	55	38	7.4	20.8	21.9	42	6	7
O35	13.51	8.31	19	10	1.9	4.4	27.6	20	2.8	1
O36	31.66	10.16	57	46	8.3	27	26.8	53	8.6	8
O37	9.1	6.93	7	5	0.9	1.5	2.9	6	1.7	3
O38	7.45	5.81	4	4	0.7	1.1	2.1	5	2	2
O39	30.22	10.14	53	43	8.3	27.5	27.1	52	8.1	8
O40	6.43	4.56	4	3	0.6	0.7	3.9	5	1.4	0.5
O41	27.33	9.11	35	27	5.3	16.8	20.6	36	6.3	6
O42	6.11	4.41	6	5	1.1	2.1	3.2	6	2.6	1
O43	33.67	10.2	51	41	8	28.3	28.6	54	8.4	7
O44	12.84	8.56	24	18	3.4	9.3	9.3	20	4.4	4
O45	14.66	8.67	27	19	4	10.9	11.7	24	3.9	3
O46	28.95	9.51	48	33	6	16.1	15.2	32	5.2	6
O47	5.64	3.32	11	7	1.1	2	2.1	7	1.9	1

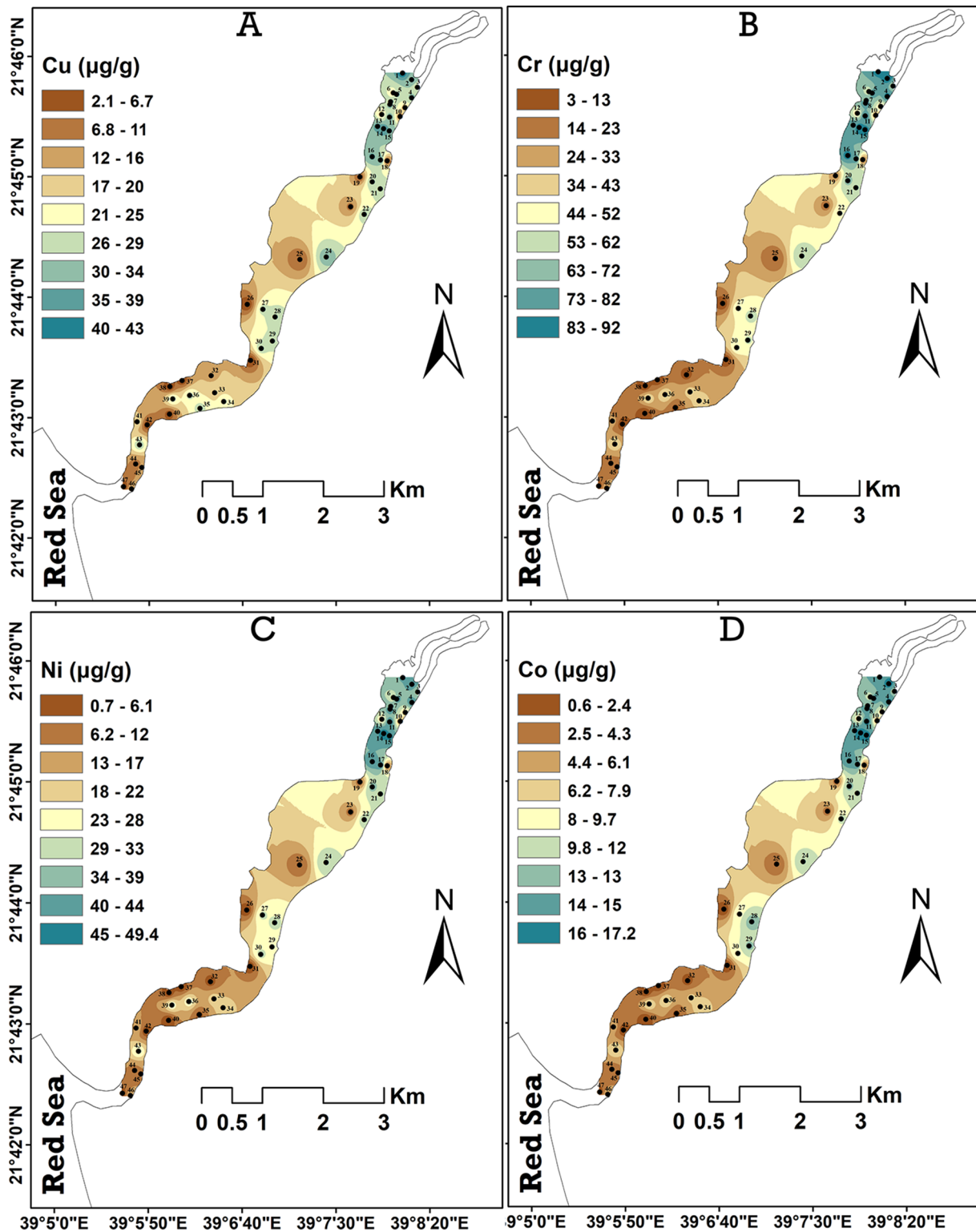


Fig. 4 Spatial distribution maps for the Copper, Chromium, Nickel, and Cobalt concentrations in the Sharm Obhur site

4.4 Benthic Ostracoda Distribution, Abundance, and Diversity

Seventy ostracod species belonging to 42 genera, were

recorded in Sharm Obhur, out of which 19 species were found to be alive (Appendix 1). The dominant genera are *Xestoleberis*, *Pontoparta*, *Cyprideis*, and *Cytherella*, which attain 19.9%, 10%, 7.7% and 6.1% of the recorded fauna,

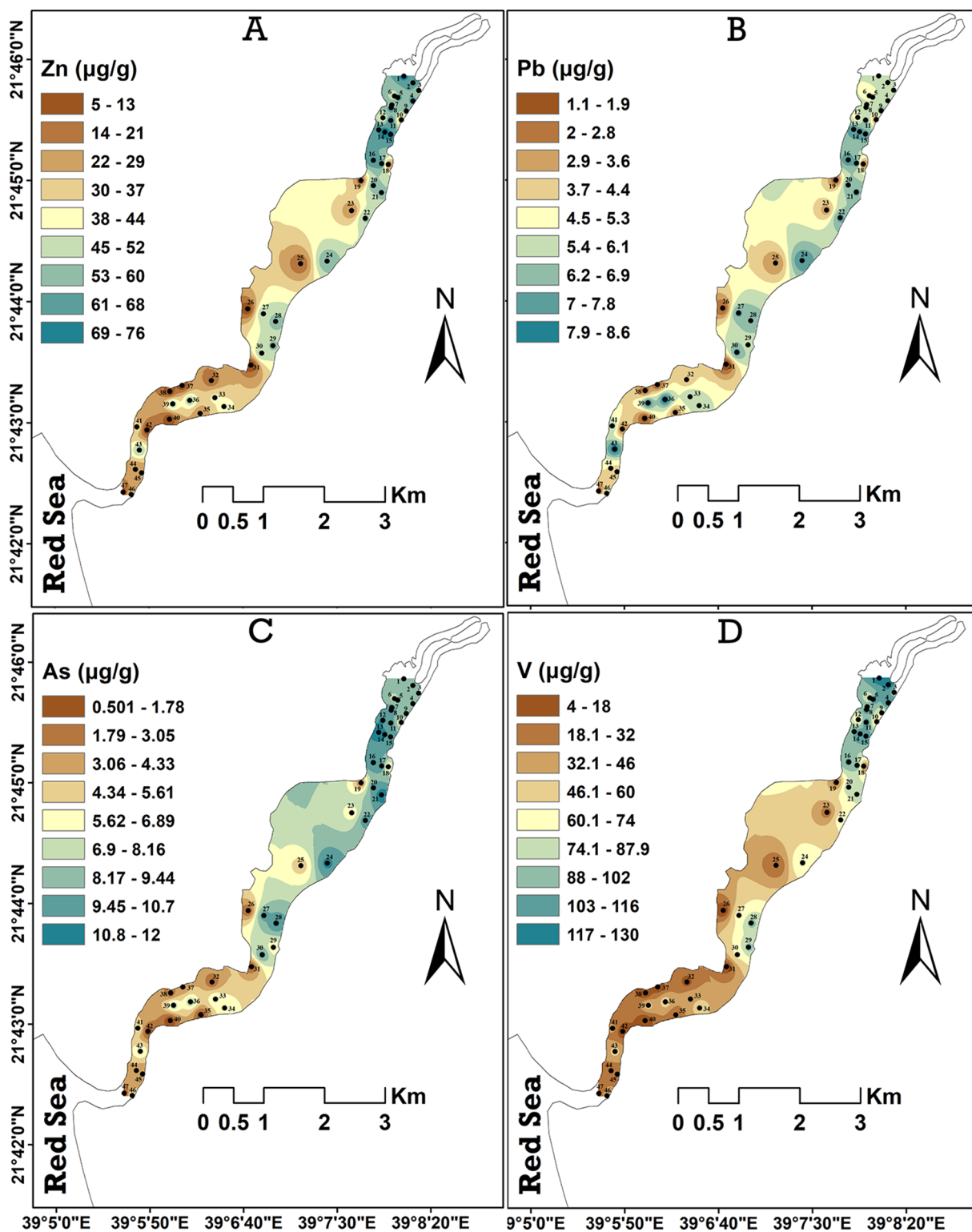
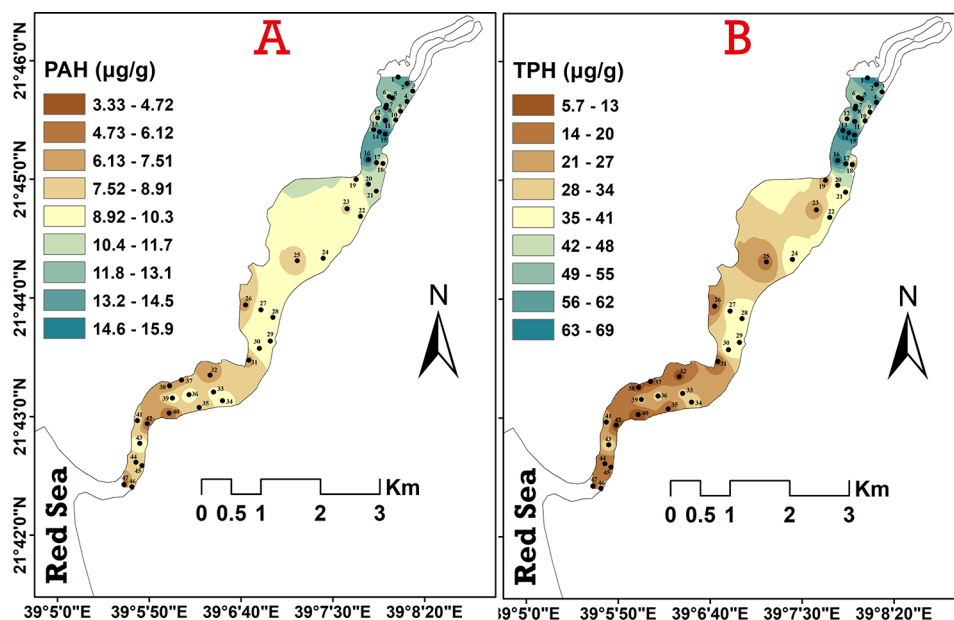


Fig. 5 Spatial distribution maps for the Zinc, Lead, Arsenic, and Vanadium concentrations in the Sharm Obhur site

Fig. 6 Spatial distribution maps of organic pollutant concentrations (Total Petroleum Hydrocarbon TPH, and Polycyclic Aromatic Hydrocarbons PAHs) for Sharm Obhur sediments



respectively. The other recorded genera are as follows; *Moosella* (5.9%), *Loxocorniculum* (~5.5%), *Ruggieria* (4.8%), *Hemicytheridea* (4.6%), *Lankacythere* (4.2%), *Miocyprideis* (2.9%), *Alocopocythere* (2.8%), and *Paranesidea* (2.7%) (Appendix 1).

Cyprideis torosa, *Ruggieria danielopoli*, *Loxocorniculum ghardaquensis*, *Moosella striata*, *Pontoparta salina* and *Alocopocythere reticulata* are the most occurring ostracod taxa observed alive and dead in the Sharm Obhur stations, respectively. They accounted for over 70% of the total assemblage of living ostracods, while the other living taxa signify less than 30% (Appendix 1). Figure 7 illustrates the overall distribution pattern of the six most abundant ostracod taxa. *Cyprideis torosa* relative abundance is averaging ~15% in the investigated stations, where it exhibits the highest occurrences with a significant proliferation at station O11 (~39%), while the lowest values (0%) observed at stations O12, O19, O21, O38, and O39 (Fig. 7A). Overall, the *C. torosa* pattern indicates that the majority of station values ranges between 12.5% and 18% relative abundance. Secondly, *R. danielopoli* is the second most abundant taxon. In the sharm head stations, it displays lower relative abundance values compared to the sharm entrance stations (Fig. 7B). It is averaging 9.7%, where the highest value was observed at station O21 (~21%), while zero value was recorded at stations O9-O12, O15-O16 (Fig. 7B). The distribution of *L. ghardaquensis* and *M. striata* fluctuate across most of the sharm stations, with average 8.5, and 8.4 respectively (Fig. 7C and D). The highest values were observed beyond stations O21 (20%), and O23 (~16%), while zero value was obtained beyond the sharm head stations, including O5-O7, O10-O12, and O8-O9, and O11, respectively (Fig. 7C and D). Additionally, the sharm head stations exhibited a higher

frequency of zero abundance values for these two taxa compared to the sharm entrance stations. The relative abundance of the *P. salina*, and *A. reticulata* leaped sharply at stations O17 (35%), and O11(45%), respectively (Fig. 7E and F). The sharm head stations had higher percentages of *A. reticulata* compared to the sharm entrance stations (Fig. 7E and F). On the other hand, *P. salina* displayed comparable relative abundance between the sharm head and entrance stations.

The spatial distribution percentage of the living ostracod taxa in the sharm head stations is quite low (Fig. 8A). The highest living ostracod percentage was observed beyond station O47 (~37.3%) at the sharm entrance, whereas the lowest percentages were observed at stations O11, and O16 (0%), followed by O15 (5.8%), O10 (6%), and O8 (~6.5%) (Fig. 8A). The stations located in the sharm head exhibited a lower percentage of living ostracod abundance in comparison to the stations located at the entrance of the sharm (Fig. 8A). They are dominated by *A. reticulata*, and *H. paiki*, while the other ostracod taxa were in dead form. On the other hand, the stations located beyond the head of the sharm displayed low living *C. torosa* % (Fig. 8B) and increases toward the sharm entrance stations. The distribution pattern of the *C. torosa* is comparable to the stations closer to the pollution sources (i.e., O11, and O16) where displayed disappearances of the *C. torosa* and most of the living ostracods species except *H. paiki* and *A. reticulata*.

Overall, the ostracod abundance is high in most stations except stations located at the sharm head as shaded in the two polygons (Fig. 9A). Two groups I, and II are displaying two degrees and levels of species abundance and richness. The stations belong to group I showed lower species abundance and richness than group II (Fig. 9A). Stations O37 and O47 display the highest ostracod abundance and

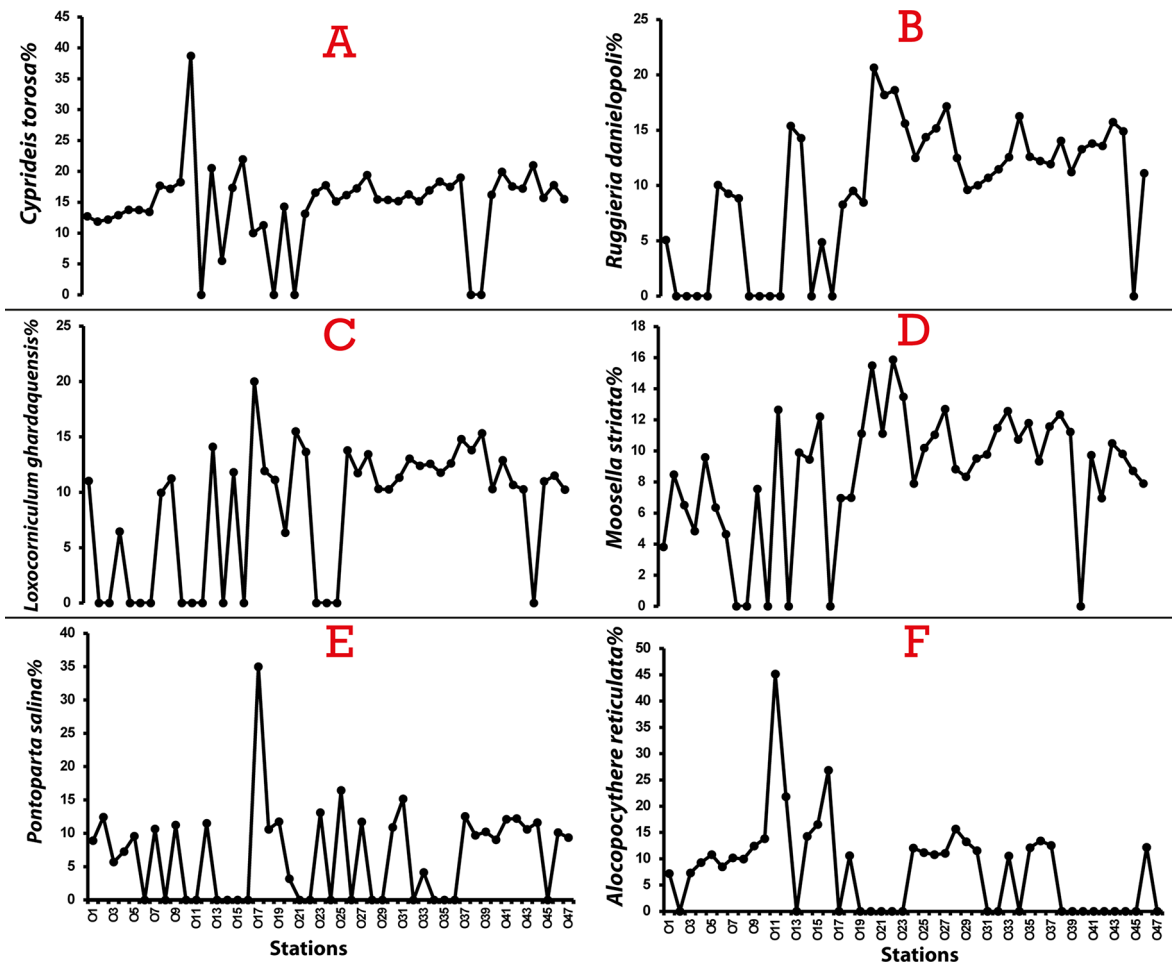
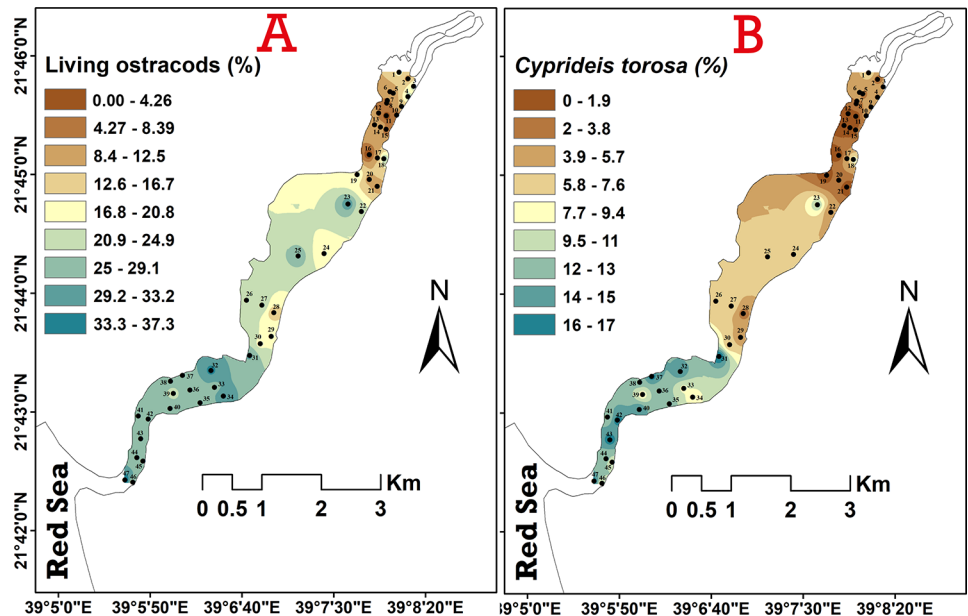


Fig. 7 The distribution of the six most dominant ostracod taxa; **A- *Cyprideis torosa***, **B- *Ruggieria danielopoli***, **C- *Loxocorniculum ghardaquisis***, **D- *Moosella striata***, **E- *Pontoparta salina***, and **F- *Alococythere reticulata***

Fig. 8 **A** Spatial distribution map for the living ostracod percentages retrieved from the Sharm Obhur stations, **B** Spatial distribution map for the highest living ostracod percentages (*Cyprideis torosa*)



richness (313, and 15; respectively), while station O11 shows the lowest species abundance and richness (25, and 3; respectively). Moreover, station O11 is dominated by *H. paiki*, and *A. reticulata*. The dominance index of O11 is the highest (0.37), while O1 shows the lowest (0.08), whereas the Shannon index was 1.03, and 2.58 for the two stations, respectively (Fig. 9B).

4.5 Statistical Analyses

4.5.1 Hierarchical Cluster Analysis (HCA)

The HCA reveals distinct clusters as shown in Fig. 10. They are characterized by different environmental biotopes and degrees of pollution. Q-mode cluster analysis was performed to study similarities between the stations. Samples are grouped into two main clusters (Q1 and Q2), each with two subclusters occupied by distinctive ostracods assemblage (Fig. 10A and B).

Cluster Q1 consists of two subclusters; they are Q11, and Q12. The subcluster Q11 is represented by twelve stations: O1, O2, O3, O4, O5, O6, O7, O8, O9, O10, O15, and O20 (Fig. 10A). These stations are in the vicinity of the head of the Sharm Obhur, where the wadi deposits are dominated. This subcluster is characterized by a high abundance of benthic ostracods assemblage comprised of *Lankacythere elaborata*, *Miocyprideis spinulosa*, *Loxococoncha ornativalvae*, *Cytherella punctata*, *Xestoleberis rhomboidea* (Fig. 10B).

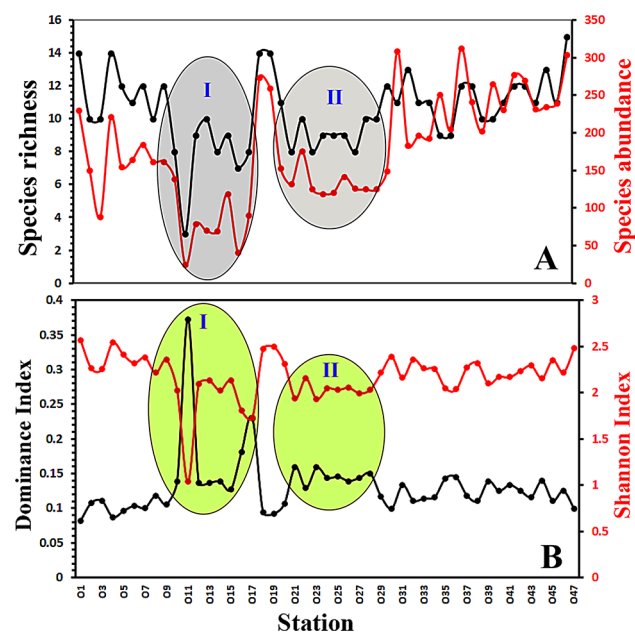


Fig. 9 A- Species richness and abundance (number of the counted individuals per 20 gram/ dry weight) of the total living ostracod assemblages retrieved from the studied stations, B- Diversity indices (Shannon and Dominance) for the total living ostracod assemblages in the investigated stations. Note, the shaded polygons show the highest impacted stations

The second subcluster (Q12) includes eighteen stations (O11, O12, O13, O14, O16, O17, O21, O22, O23, O24, O25, O26, O27, O28, O29, O30, O33, and O36) (Fig. 10A). These stations are located directly beside the touristic hotels and marinas, where highest concentrations of heavy metals, and TOM% were observed. This subcluster is signified by having low to moderate species abundance and richness. The prevailing ostracod assemblage in this subcluster is defined by occurrence of *A. reticulata* (Fig. 10B).

Cluster Q2 is subdivided into two subclusters Q21, and Q22 (Fig. 10A). Subcluster Q21 is discriminated by an ostracod assemblage that includes *L. arenicola*, *M. striata*, *L. ghardaqensis*, *R. danielopoli*, and *Jugosocythere borchersi*. It consists of thirteen stations: O18, O19, O31, O32, O34, O35, O37, O38, O39, O40, O43, O46, and O47 (Fig. 10A). These stations are located near the entrance of the sharm, where they display high species abundance and richness. The heavy metals contents are low to moderate concentrations, while carbonate percentages are high.

Subcluster Q22 comprises three stations: O35, O37, and O46, where they are occupying the southwestern sector of the Sharm Obhur. This subcluster has an assemblage consisting of *Tanella gracilis*, *P. fracticorallicola*, *Callistocythere arcuata*, *P. salina*, *Xestoleberis rotunda*, *Loxococoncha gurneyi*, *C. torosa*, and *H. paiki* (Fig. 10B). This assemblage exhibits high species richness and abundance.

4.5.2 Redundancy Analysis (RDA)

The results of the Redundancy Analysis (RDA) are visualized in Fig. 11. The first two dimensions of the RDA explain 73.48% of the total variance for ostracod relative abundances and environmental data. Most of the variability (59.75%) can be attributed to the influence of heavy metals, and organic pollutants which have emerged as the most significant factors in shaping the community structure of ostracods in the study area (Fig. 11). It is worth noting that the concentrations of heavy metals exhibit a negative correlation with living ostracod abundance and diversity, whereas a positive correlation is observed with the dead ostracod percentage (Fig. 11). For that, two main groups are discriminated based on the response of ostracods to heavy metals and environmental parameters. Group I is mostly occupied by the sharm head stations (Fig. 11). These stations render low species diversity and abundances, for instance O11, and O16 (see; Fig. 8). Moreover, these stations displayed the highest organic pollutants (TPH, and PAH), heavy metals, mud%, and TOM%. Interestingly, this group is occupied by only two benthic ostracods taxa: *H. paiki*, and *A. reticulata*. The zone of moderate heavy metals concentrations has a benthic ostracod assemblage comprised of *L. ornativalvae*, *M. spinulosa*, *C. punctata*, and *L. elaborata*. Group

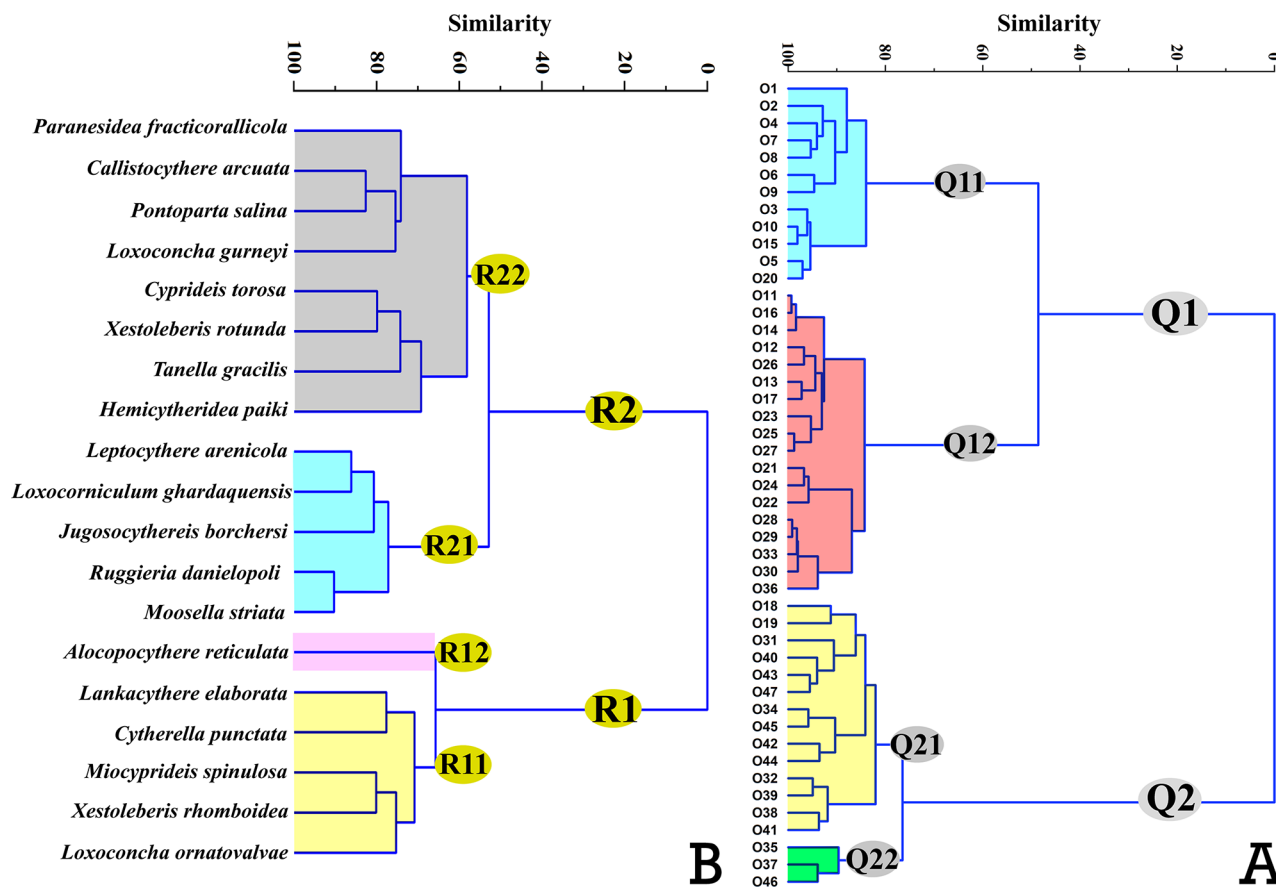


Fig. 10 Dendrograms for hierarchical cluster analysis (HCA) on the benthic ostracod > 2% based on R- and Q modes using Euclidean dissimilarity index

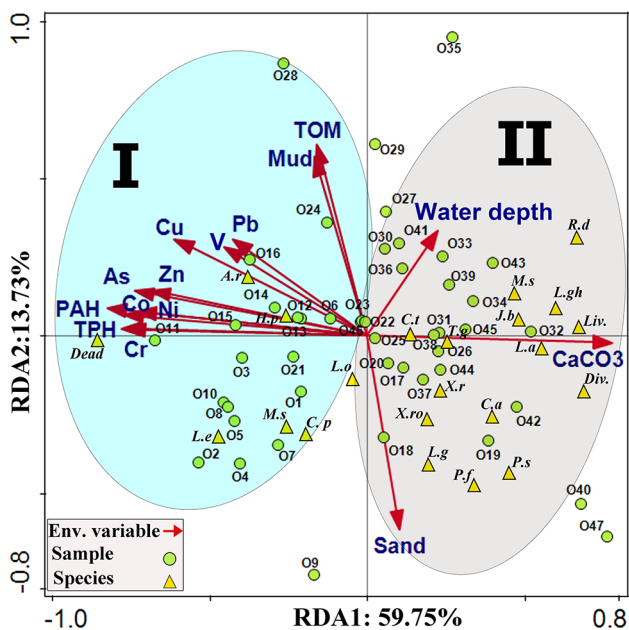


Fig. 11 Triplot redundancy analysis (RDA) of the highest occurrences benthic ostracods association and their controlling environmental factors for the investigated stations

II involves most of the stations located at the entrance of the Sharm Obhur with emphasis on the controlling factors responsible for their distribution. These factors are the sand%, CaCO₃%, and water depth, where they redistribute the ostracods biofacies. Most of ostracod species and living percentages are positively correlated with the group II stations, where the carbonate content is the main controlling factor. The dominant ostracod assemblage in this group includes *X. rotunda*, *X. rhomboidea*, *P. salina*, *P. fracticorallicola*, *C. arcuata*, *L. arenicola*, *C. torosa*, *T. gracilis*, *M. striata*, *L. ghardaquensis*, *R. danielopoli*, and *J. borchersi*.

4.5.3 Cross-Plot Analysis

Figure 12 displays cross-plot analysis between TOM content and selected ostracod dominant taxa. The *H. paiki* and *A. reticulata* occurrences exhibited a strong positive correlation coefficient in the stations highly enriched by TOM ($R^2=0.83$, $p<0.05$) and ($R^2=0.67$, $p<0.05$), respectively (Fig. 12). Conversely, the abundances of *P. salina*, *M. striata*, *C. torosa*, *X. rotunda* and *L. ghardaquensis* showed negative correlation coefficients with TOM content (Fig. 12). These species displayed a decreasing trend with high TOM content

which may indicate a direct influence by organic matter. On the other hand, although TOM content is often influenced by grain size, our study reveals strong positive correlation coefficients between TOM content and stations dominated by high mud% ($R^2=0.88, p < 0.05$), while a strong negative correlation between TOM and stations controlled by high sand% ($R^2= -0.84, p < 0.05$) (Fig. 12).

5 Discussion

5.1 Distribution, Diversity Indices, and Abundance of Ostracod Assemblage

Benthic ostracod distribution is controlled by many factors, such as bottom substrate characteristics (Helal and Abd El-Wahab 2012; El-Kahawy et al. 2021). The recorded ostracod taxa in Sharm Obhur are dominated by the phytal, and shallow marine assemblage. These species are all commonly found in the Red Sea along the Egyptian and Saudi Arabian coastlines (Hartman 1964; Bonaduce et al. 1983; Helal

and Abd El-Wahab 2004; Mohammed and Keyser 2012; Mohammed et al. 2012; Keyser and Mohammed 2021). They are living in colonies in areas of enriched seagrasses, macro-algae, and reef communities. These ecological microhabitats are favourable for various species such as *C. torosa*, *L. ghardaensis*, *R. danielopoli*, *Xestoleberis* spp., and *J. borchersi*, especially at the stations near the sharm entrance. On the other hand, the sharm head is occupied by bottom facies of mud-types (those dominated by clay particle size fraction) which lacking seagrasses and reef sediments likely due to effluent discharge from ships and touristic villages. Significantly, these conditions play a remarkable role in the decrease of living ostracod percentage of the Sharm Obhur site. Consequently, the dead ostracods are higher in the stations at the head of the sharm at the expense of living forms (i.e., *H. paiki*, and *A. reticulata*).

Species diversity is a crucial indicator for assessing the impacts of environmental stress on benthic microfauna (Ruiz 1994; El-Kahawy et al. 2021). Consequently, the abundance and diversity of ostracods undergo significant changes due to various sources of contamination (Ruiz et

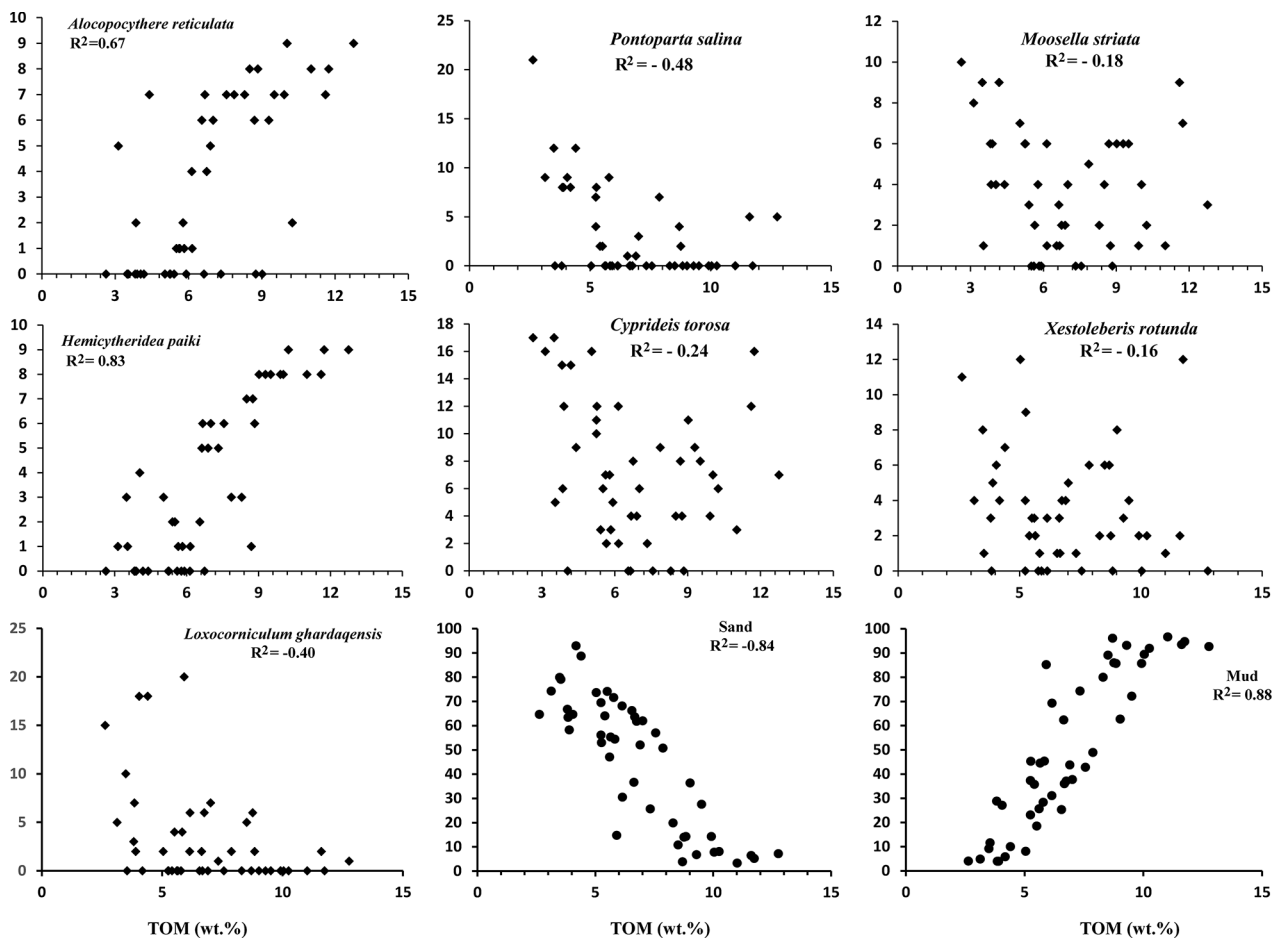


Fig. 12 Scatter-plot relationship among the dominant ostracod species and bottom facies (sand and mud%) versus total organic matter content (TOM wt%). Note r : correlation coefficient ($p < 0.05$)

al. 2013). However, certain species, such as *C. torosa* and *C. dimorpha*, exhibit resistance to organic contamination (Lim and Wong 1986), along with low species diversity in the contaminated environments (Alin et al. 1999). Several authors (e.g., Ruiz et al. 2013; El-Kahawy et al. 2021; references therein) recorded variations in species diversity as a response to contamination. They indicated that ostracods are typically scarce or absent in polluted stations from domestic sources. Additionally, Van der Merwe (2003) has inferred that mining activities have similar effects on ostracod assemblages. Nonetheless, Aiello et al. (2021) reported high diversity assemblages in marine environment with very high levels of heavy metals. Our findings indicated that the pollution affecting the marine benthic environments of the study area is not severe enough to completely eliminate ostracods, which is comparable to the results obtained by Carman et al. (2000) and Lenihan et al. (2003). Still, pollution has a significant impact on residual ostracod communities. It results in a high dominance index and low abundance, with only a few opportunistic species present (Millward et al. 2004). This relationship is clearly apparent in stations O11, O12, O13, O14, O15, O16, and O17, which exhibit the highest dominance index values, very low species abundance, and elevated concentrations of heavy metals (Fig. 9A and B). In shelf environments, species diversity increases generally with increasing water depth (Bonaduce et al. 1983; Ruiz et al. 1997). Accordingly, species diversity decreases closer to the sharm head (shallowest stations) (Fig. 9A), which may be attributed to factors such as increased heavy metals, TOM, and organic pollutants, as observed in stations O11, O12, O13, O14, O15, O16, and O17. These results are consistent with the findings of Samir (2000), that focussed on the decline of faunal diversity and abundance in the polluted areas. The observation of low ostracod abundance accompanied by moderate to high diversity, particularly in the vicinity of contaminated stations (O12, O13, and O14; see Fig. 9), aligns consistently with the findings of Liljenstroem et al. (1987).

5.2 Ostracoda Abundance and Environmental Factors

The abundance of meiofauna, including ostracoda, is influenced by the amount of organic matter preserved in sediments (Mazzola et al. 1999; Mirto et al. 2000; Lili Fauzielly et al. 2013; Irizuki et al. 2015). Irizuki et al. (2015) show a positive relationship between TOM content and ostracod abundance. On the other hand, Mirto et al. (2000) observed a decline in ostracod abundance following the establishment of fish and mussel farms, attributed to bio-deposition from the farming complexes. However, they did not investigate whether the response to organic matter was species-specific.

Lili Fauzielly et al. (2013) focused on species-specific responses and investigated the correlation between TOM content and the abundance of various ostracod species in surface sediments from enclosed seas, aiming to inspect indicator species for monitoring environmental changes. However, their study involved surface sediments from different sites, water depths, and substrates, which were influenced by various environmental factors, making it challenging to show specific relationships. They reported that a common occurrence of *Keijella carriei* and *Loxoconcha wrighti* denoted their preferability of high TOM content, while *Hemicytheridea ornata* and *Hemicytheridea reticulata* rarely occurred.

Our findings indicated that salinity, water depth, temperature, and pH exhibited limited variations and lack significant correlations with ostracod abundance. Additionally, the recognized dominant ostracod species observed were indicative of shallow marine mud habitats, which suggest that the ostracod assemblages described in this study are composed of autochthonous species. Comparing ostracod abundance with environmental factors such TOM through cross-plot analysis, may be utilized to assess ostracod species as indicators of anthropogenic influences. *A. reticulata* has been previously used as bioindicators to recognize such environments of high TOM (Helal and Abd El-Wahab 2012; El-Kahawy et al. 2021). The results of the current study support earlier findings and demonstrate that TOM content directly correlates to the abundance of the analyzed species. The enrichment of TOM content appears to be closely related to eutrophication (Malone and Newton 2020). Thus, the present work suggests that *H. paiki*, and *A. reticulata* serve as good bioindicators for organic matter enrichment via eutrophication. The *P. salina*, *M. striata*, *L. ghardaqensis*, *C. torosa* and *X. rotunda*, however, can act as good bioindicators of general environmental deterioration due to increased organic matter in sediments. Moreover, the positive relationship between bottom facies, particularly mud, suggests a significant influence of the enriched TOM, along with TPH, PAHs, and heavy metals especially at the head of the Sharm Obhur.

5.3 Heavy Metals

The relationship between heavy metal pollution and ostracods abundance has been discussed by several authors (Pascual et al. 2002; Yasuhara et al. 2003, 2012; Lee and Correa 2005; Bergin et al. 2006; Ruiz et al. 2008; Irizuki et al. 2011, 2018; El-Kahawy et al. 2021). These studies have consistently shown that increased concentrations of Cu and/or Zn are associated with a decline in ostracods abundance, leading to their retreat or even disappearance in highly polluted areas. Yasuhara et al. (2003) documented

that *Bicornucythere bisanensis* exhibits a robust resistance to anthropogenic pollutants, whereas *Callistocythere alata* exhibits sensitive behaviour to pollution. In a study by Rahman and Ishiga (2012), trace elements were examined to inspect their influence on the ostracods abundance and showed a lowering in ostracods abundance when the heavy metals concentration increased. Interestingly, various pollution sources have been found to significantly impact both the species abundance and diversity of ostracods. Specifically, in areas characterized by high organic pollution resulting from urban or industrial activities, ostracods are typically scarce and may even vanish entirely (Poquet et al. 2008). Similarly, mining activities have been observed to display comparable effects on ostracod assemblages, with a rapid decline in species abundance near polluted areas (Van der Merwe 2003). Noteworthy that the concentrations of the analyzed heavy metals (Zn, Cr, Ni, Cu, Co, V, Pb, and As) in the present study are significantly high, particularly in the sharm head stations. Furthermore, their contributions are notably greater than those reported by Basaham et al. (2006), and Ghandour et al. (2014) in the study area. Similar to El-Kahawy et al. (2021), our results suggest a short-term increase in the content of these elements in the shallow marine sediment of the Red Sea. Of particular concern, the remarkably high contribution of As, and Pb in the sharm head stations of our study, exceeds the average levels of Ghandour et al. (2014) found in shallow marine sediment and potentially poses ecosystem hazards. This partly clarifies the trend of ostracod abundance, and diversity in the stations at the sharm head, where a high TPH, PAHs, heavy metals, and organic matter contents were recorded, especially around stations O11, O12, O1, O14, O15, O16, and O17. Field observation confirms that shipping, along with anthropogenic activities, constitute the main sources of pollution in the Sharm Obhur site.

6 Conclusion

This study investigated the bottom sediments of Sharm Obhur, near Jeddah, Kingdom of Saudi Arabia, focusing on the influence of heavy metals, and organic pollutants on benthic ostracods assemblage. The integrated findings of benthic ostracod occurrences, geochemical data, and statistical analyses highlight the potential of *H. paiki* and *A. reticulata* as effective bio-monitors for the polluted stations. Furthermore, the study revealed that certain species, such as *L. ghardaqensis*, *C. torosa*, *M. striata*, *X. rotunda*, and *X. rhomboidea* were less abundant in the contaminated stations, indicating their lower tolerance to the heavily pollution areas. Additionally, the study reported that the abundance of living benthic forms was limited in the head of the

sharm stations, potentially due to unfavourable environmental conditions. However, the entrance of the sharm exhibited a higher level of biodiversity among benthic ostracods, indicating a more favourable and diverse habitat. Also, the multivariate statistical (RDA) relationships elaborated that *H. paiki* and *A. reticulata* are positively related, which means that they are likely to be able to survive in stations with a high TOM%, while the other dominant taxa were negatively related. These findings contribute to our understanding of the ecological implications of pollution on benthic ostracods and emphasize the importance of using certain ostracods species of moderately polluted environments as bioindicators for monitoring and assessing environmental contamination. Further research is encouraged to expand our knowledge of the sources, transport, and ecological effects of heavy metal contamination on biodiversity (i.e., ostracods, corals, etc.) in the Sharm Obhur site, to inform local and regional environmental management as well as to best calibrate the use of these bioindicators elsewhere in the broader region and, potentially, globally.

Supplementary Information The online version contains supplementary material available at <https://doi.org/10.1007/s41748-024-00459-0>.

Acknowledgements This research work was funded by the Institutional Fund Projects under grant no. IFPHI-291-980-2020. The authors gratefully acknowledge technical and financial support from the Ministry of Education and King Abdulaziz University, DSR, Jeddah, Saudi Arabia. The authors wish to express their deep gratitude to the editor and reviewers for their constructive comments and editorial handling.

Author Contributions MA, RE, IG; conceptualization, methodology, formal analysis, writing original draft, writing review, and editing. ME, BA: formal analysis, writing original draft. AQ; writing, reviewing, and editing, FA, MA, IG; field sampling, methodology, supervision. All authors have read and agreed to the final manuscript.

Funding This work is funded by the Ministry of Education and King Abdulaziz University under project grant no. 291-980-2020.

Data Availability Upon request, interested individuals can obtain the data outlined in this study by contacting the corresponding author.

Declarations

Ethical Approval Not applicable.

Consent to Participate Not applicable.

Conflict of Interest The authors declare that they have no known competing financial interests or personal relationships that could have appeared to influence the work reported in this paper.

References

- Abdel-Shafy HI, Mansour MS (2016) A review on polycyclic aromatic hydrocarbons: source, environmental impact, effect on human health and remediation. *Egypt J Pet* 25(1):107–123
- Ahmad F, Sultan SA (1993) Tidal and sea level changes at Jeddah, Red Sea. *Pak J Mar Sci* 2(2):77–84
- Aiello G, Amato V, Barra D, Caporaso L, Caruso T, Giaccio B, Parisi R, Rossi A (2020) Late quaternary benthic foraminiferal and ostracod response to palaeoenvironmental changes in a Mediterranean coastal area, Port of Salerno, Tyrrhenian Sea. *Reg Stud Mar Sci* 40:101498
- Aiello G, Barra D, Parisi R, Arienzo M, Donadio C, Ferrara L, Toscanesi M, Trifuoggi M (2021) Infralittoral ostracoda and benthic foraminifera of the Gulf of Pozzuoli (Tyrrhenian Sea, Italy). *Aquat Ecol* 55(3):955–998
- Al-Farawati R, El Sayed MAK, Rasul NM (2019) Nitrogen, phosphorus and organic carbon in the Saudi Arabian Red Sea Coastal Waters: behaviour and human impact. *Oceanographic and Biological Aspects of the Red Sea*, pp 89–104
- Alin S, Cohen AS, Bills R, Mukway M, Michel M, Tiercelin K, Couvellers P, Keita S, West K, Soreghan M, Kimbadi S, Ntakimazi G (1999) Effects of landscape disturbance on animal communities in Lake Tanganyika, East Africa. *Conserv Biol* 13:1017–1033
- Alsaafani MA, Alraddadi TM, Albarakati AM (2017) Seasonal variability of hydrographic structure in Sharm Obhur and water exchange with the Red Sea. *Arab J Geosci* (10): 1–10
- Anadón P, Gliozzi E, Mazzini I (2002) Paleoenvironmental reconstruction of marginal marine environments from combined paleoecological and geochemical analyses on ostracods. *Ostracoda: Appl Quaternary Res* 131:227–247
- Badr NB, El-Fiky AA, Mostafa AR, Al-Mur BA (2009) Metal pollution records in core sediments of some Red Sea coastal areas, Kingdom of Saudi Arabia. *Environ Monit Assess* 155:509–526
- Bantan RA, Ghandour IM, El-Kahawy RM, Aljhdali MH, Althagafi AA, Al-Mur BA, Quicksall AN (2024) Environmental assessment of toxic heavy metals in bottom sediments of the Sharm Obhur, Jeddah, Saudi Arabia. *Mar Pollut Bull* 205:116675. <https://doi.org/10.1016/j.marpolbul.2024.116675>
- Barras C, Jorissen FJ, Labrune C, Andral B, Boissery P (2014) Live benthic foraminiferal faunas from the French Mediterranean Coast: towards a new biotic index of environmental quality. *Ecol Indic* 36:719–743
- Basaham AS, El-Shater A (1994) Textural and mineralogical characteristics of the surficial sediments of Sharm Obhur, Red Sea coast of Saudi Arabia. *J King Abdulaziz Univ Mar Sci* (5): 51–71
- Basaham AS, Rifaat AE, El-Sayed MA, Rasul N (2006) Sharm Obhur: environmental consequences of 20 years of uncontrolled coastal urbanization. *J King Abdulaziz Univ Mar Sci* 17(1):129–152
- Bergin F, Kucuksezgin F, Uluturhan E, Barut IF, Meric E, Avsar N, Nazik A (2006) The response of benthic Foraminifera and Ostracoda to heavy metal pollution in Gulf of Izmir. *Estuar Coast Shelf Sci* 66:368–386
- Bodergat AM, Bonnet L, Colin JP, Cubaynes R, Rey J (1998) Opportunistic development of *Ogmoconcha amalthei* (ostracod) in the lower Liassic of Quercy (SW France): an indicator of sedimentary disturbance. *Palaeogeogr Palaeoclimatol Palaeoecol* 143(1–3):179–190
- Bonaduce G, Masoli M, Pugliese N (1976) Ostracoda from the Gulf of Aqaba (Red Sea). *Pubbl Staz Zool Napoli* 40(2):372–428
- Bonaduce G, Masoli M, Minichelli G, Pugliese N (1980) Some new benthic marine ostracoda species from the Gulf of Aqaba (Red Sea). *Bull Soc Paleont Ital* 19(1):143–178
- Bonaduce G, Ciliberto B, Minichelli G, Masoli M, Pugliese N (1983) The Red Sea benthic ostracodes and their geographical distribution. *Proceedings of the 8th International Symposium on Ostracoda: Applications of Ostracoda*, (R. F. Maddocks, ed.) Univ. Houston Geosc, pp 472–491
- Boomer I, Eisenhauer G (2002) Ostracod faunas as palaeoenvironmental indicators in marginal marine environments. In: Holmes JA, Chivas AR (eds) *The Ostracoda: applications in Quaternary Research*. *Geophys Monogr Ser* 131. AGU, Washington, DC, pp 135–149
- Bouchet VM, Alve E, Rygg B, Telford RJ (2012) Benthic foraminifera provide a promising tool for ecological quality assessment of marine waters. *Ecol Indic* 23:66–75
- Carman KR, Todaro MA (1996) Influence of polycyclic aromatic hydrocarbons on the meiobenthic-copepod community of a Louisiana salt marsh. *J Exp Mar Bio Ecol* 198(1):37–54
- Carman KR, Fleegeer JW, Pomarico SM (2000) Does historical exposure to hydrocarbon contamination alter the response of benthic communities to diesel contamination? *Mar Environ Res* 49:255–278
- Cibic T, Franzo A, Celussi M, Fabbro C, Del Negro P (2012) Benthic ecosystem functioning in hydrocarbon and heavy-metal contaminated sediments of an Adriatic lagoon. *Mar Ecol Prog Ser* 458:69–87
- Dean WE (1974) Determination of carbonate and organic matter in calcareous sediments and sedimentary rocks by loss in ignition: comparison with other methods. *J Sedimen Petrol* 44:242–248
- Eagar SH (1999) Distribution of Ostracoda around a coastal sewer outfall: a case study from Wellington, New Zealand. *J Royal Soc New Z* 29:257–264
- Eek E, Cornelissen G, Kibsgaard A, Breedveld GD (2008) Diffusion of PAH and PCB from contaminated sediments with and without mineral capping; measurement and modelling. *Chemosphere* 71(9):1629–1638
- El Nemr A, El-Sadaawy MM, Khaled A, El-Sikaily A (2014) Distribution patterns and risks posed of polycyclic aromatic hydrocarbons contaminated in the surface sediment of the Red Sea coast (Egypt). *Desalin Water Treat* 52(40–42):7964–7982
- El-Kahawy R, El-Shafeiy M, Helal S, Aboul-Ela N, Abd El-Wahab M (2021) Benthic ostracods (crustacean) as a nearshore pollution bio-monitor: examples from the Red Sea Coast of Egypt. *Environ Sci Pollut Res* 28:31975–31993
- Folk RL, Ward WC (1957) Brazos River bar: a study in the significance of grain size. *J Sediment Petrol* 27(1):3–26
- Ghandour IM, Basaham S, Al-Washmi A, Masuda H (2014) Natural and anthropogenic controls on sediment composition of an arid coastal environment: Sharm Obhur, Red Sea, Saudi Arabia. *Environ Monit Assess* 186:1465–1484
- Ghetti PF (1980) Biological indicators of the quality of running waters. *Ital J Zool* 47(3–4):381–390
- Goswami P, Ohura T, Guruge KS, Yoshioka M, Yamanaka N, Akiba M, Munuswamy N (2016) Spatio-temporal distribution, source, and genotoxic potential of polycyclic aromatic hydrocarbons in estuarine and riverine sediments from southern India. *Ecotoxicol Environ Saf* 130:113–123
- Gross MG (1971) Carbon determination. In: Carver RE (ed) *Procedures in Sedimentary Petrology*. Wiley, New York, pp 573–596
- Hammer Ø, Harper DAT, Ryan PD (2009) *PAST-Palaeontological Statistics 1.89*. Univ. of Oslo, Oslo: 1–31
- Hartmann G (1964) Neontological and paleontological classification of Ostracoda. Ostracods as ecological and palaeoecological indicators. *Pubbl Stn Zool Napoli* 33:550–587
- Hees W (1977) Sewage discharges from ships transiting coastal salt waters. *J Am Water Resour Assoc* 13(2):215–230
- Helal S, Abd El-Wahab M (2004) Recent ostracodes from marine sediments of Safaga Bay, Red Sea, Egypt. *Egypt J Paleontol* 4:75–93

- Helal S, Abd El-Wahab M (2012) Distribution of podocopid ostracods in mangrove ecosystems along the Egyptian Red Sea coast. *Crustaceana* 85(14):1669–1696
- Irizuki T, Takimoto A, Sako M, Nomura R, Kakuno K, Wanishi A, Kawano S (2011) The influences of various anthropogenic sources of deterioration on meiobenthos (Ostracoda) over the last 100 years in Suo-Nada in the Seto Inland Sea, Southwest Japan. *Mar Pollut Bull* 62:2030–2041
- Irizuki T, Ito H, Sako M, Yoshioka K, Kawano S, Nomura R, Tanaka Y (2015) Anthropogenic impacts on meiobenthic Ostracoda (Crustacea) in the moderately polluted Kasado Bay, Seto Inland Sea, Japan, over the past 70 years. *Mar Pollut Bull* 91(1):149–159
- Irizuki T, Hirose K, Ueda Y, Fujihara Y, Ishiga H, Seto K (2018) Ecological shifts due to anthropogenic activities in the coastal seas of the Seto Inland Sea, Japan, since the 20th century. *Mar Pollut Bull* 127:637–653
- Jeffrey A, Saitas PE (2001) Total Petroleum Hydrocarbons TNRCC (Texas Natural Resource Conservation Commission) Method 1005, Revision 03
- Johnsen AR, Winding A, Karlson U, Roslev P (2002) Linking of microorganisms to phenanthrene metabolism in soil by analysis of ¹³C-labeled cell lipids. *Appl Environ Microbiol* 68(12):6106–6113
- Keyser D, Mohammed M (2021) Taxonomy of recent shallow marine ostracods from Al-Hudeida City-Yemen. *Mar Micropaleontol* 164:101974
- Külköylüoğlu O, Yağcı A, Erbatur İ, Yağcı MA, Bulut C, Çınar Ş, Isparta (2023) Turkey) *Biol* 78(3): 755–769
- Kumar S, Prasad S, Yadav KK, Shrivastava M, Gupta N, Nagar S, Bach QV, Kamyab H, Khan SA, Yadav S, Malav LC (2019) Hazardous heavy metals contamination of vegetables and food chain: role of sustainable remediation approaches-A review. *Environ Res* 179:108792
- Law JB, Whinnet JA (1992) Polycyclic Aromatic Hydrocarbons in the Muscle Tissues of Harbour Porpoise from UK waters. *Mar Poll Bull* 11:550–553
- Lee MR, Correa JA (2005) Effects of copper mine tailings disposal on littoral meiofaunal assemblages in the Atacama region of northern Chile. *Mar Environ Res* 59(1):1–18
- Lenihan HS, Peterson CH, Kim SL, Conlan KE, Fairey R, McDonald C, Grabowski JH, Oliver JS (2003) Variation in marine benthic community composition allows discrimination of multiple stressors. *Mar Ecol Prog Ser* 261:63–73
- Liang M, Liang H, Rao Z, Xu D (2020) Occurrence of polycyclic aromatic hydrocarbons in groundwater from rural areas in eastern China: spatial distribution, source apportionment and health cancer risk assessment. *Chemosphere* 259:127534
- Lili Fauzielly, Irizuki T, Sampei Y (2013) Spatial distribution of recent ostracode assemblages and depositional environments in Jakarta Bay, Indonesia, with relation to environmental factors. *Paleontol Res* 16:267–281
- Liljenstroem S, Widbom B, Mattson J (1987) Effects of two oil refinery effluents on benthic Meiofauna in Mesocosms. Swedish Environmental Research Institute, p 38
- Lim RP, Wong MC (1986) The effects of pesticides on the population dynamics and production of *Stenocypris major* Baird (Ostracoda) in rice fields. *Archiv Hydrobiol* 106:421–427
- Liu WX, Wang Y, He W, Qin N, Kong XZ, He QS, Yang B, Yang C, Jiang YJ, Jorgensen SE, Xu FL (2016) Aquatic biota as potential biological indicators of the contamination, bioaccumulation and health risks caused by organochlorine pesticides in a large, shallow Chinese lake (Lake Chaohu). *Ecol Indic* 60:335–345
- Lu Y, Yuan J, Lu X, Su C, Zhang Y, Wang C, Cao X, Li Q, Su J, Ittekkot V, Garbutt RA (2018) Major threats of pollution and climate change to global coastal ecosystems and enhanced management for sustainability. *Environ Pollut* 239:670–680
- Malone TC, Newton A (2020) The globalization of cultural eutrophication in the coastal ocean: causes and consequences. *Front Mar Sci* 7:670
- Mandura AS (1997) A mangrove stand under sewage pollution stress: Red Sea, vol 1. *Mangroves and Salt marshes*, pp 255–262
- Martens K, Horne DJ (2009) Ostracoda. *Encyclopedia of inland waters*, 405–414
- Mazzola A, Mirto S, Danovaro R (1999) Initial fish-farm impact on meiofaunal assemblages in coastal sediments of western Mediterranean. *Mar Pollut Bull* 38:1126–1133
- Millward RN, Carman KR, Fleegeer JW, Gambrell RP, Portier R (2004) Mixtures of metals and hydrocarbon elicit complex responses by a benthic invertebrate community. *J Exp Mar Biol Ecol* 310:115–130
- Mirto S, La Rosa T, Danovaro R, Mazzola A (2000) Microbial and meiofaunal response to intensive mussel-farm biodeposition in coastal sediments of the western Mediterranean. *Mar Pollut Bull* 40:244–252
- Mohammed M, Keyser D (2012) Recent ostracods from the tidal flats of the coast of Aden City, Yemen. *Mar Biodivers* 42:247–280
- Mohammed M, Al -Wosabi M, Keyser D, Al-Kadasi WM (2012) Distribution and taxonomy of shallow marine ostracods from Northern Socotra Island (Indian Ocean)-Yemen. *Rev Micropaleontol* 55(4):149–170
- Monier MN, Soliman AM, Al-Halani AA (2023) The seasonal assessment of heavy metals pollution in water, sediments, and fish of grey mullet, red seabream, and sardine from the Mediterranean coast, Damietta, North Egypt. *Reg Stud Mar Sci* 57:102744
- Moore RC (1961) Treatise on invertebrate paleontology, Part Q, Arthropoda, (Ostracoda). *Geol Soc Amer Univ Kansas*, p 422
- Mostafawi N (2003) Recent ostracods from the Persian Gulf. *Senckenb Marit* 32:51–75
- Parmar TK, Rawtani D, Agrawal YK (2016) Bioindicators: the natural indicator of environmental pollution. *Front Life Sci* 9(2):110–118
- Pascual A, Rodriguez-Lazaro J, Weber O, Jouanneau JM (2002) Late Holocene pollution in the Gernika estuary (southern Bay of Biscay) evidenced by the study of Foraminifera and Ostracoda. *Hydrobiologia* 475:477–491
- Peterson CH, Kennicutt IIMC, Green RH, Montagna P, Harper DE Jr, Powell EN, Roscigno PF (1996) Ecological consequences of environmental perturbations associated with offshore hydrocarbon production: a perspective on long-term exposures in the Gulf of Mexico. *Can J Fish Aquat Sci* 53(11):2637–2654
- Poquet JM, Mezquita F, Rueda J, Miracle AR (2008) Loss of Ostracoda biodiversity in Western Mediterranean wetlands. *Aquat Conserv Mar Freshw Ecosyst* 18:280–296
- Rahman MA, Ishiga H (2012) Trace metal concentrations in tidal flat coastal sediments, Yamaguchi Prefecture, Southwest Japan. *Environ Monit Assess* 184:5755–5771
- Rasul NMA (2015) Lagoon sediments of the Eastern Red Sea: distribution processes, pathways and patterns. In: Rasul N, Stewart I (eds) *The Red Sea*. Springer, Berlin Heidelberg, pp 281–316
- Rinderhagen M, Ritterhoff J, Zauke GP (2000) Crustaceans as bioindicators. In *Biomonitoring of Polluted Water-Reviews on Actual Topics*. Trans Tech Publications-Scitech Publications, Environ Res Forum 9: 161–194
- Ruiz F (1994) Los ostracodos del litoral de la provincia de Huelva. PhD thesis, Huelva Univ, 275 p
- Ruiz F, Gonzalez-Regalado ML, Borrego J, Morales JA (1997) The response of ostracod assemblages to recent pollution and sedimentary processes in the Huelva Estuary, SW Spain. *Sci Total Environ* 207:91–103
- Ruiz F, Abad M, Bodergat AM, Carbonel P, Rodríguez-Lázaro J, Yasuhara M (2005) Marine and brackish-water ostracods as sentinels of anthropogenic impacts. *Earth-Sci Rev* 72(1–2):89–111

- Ruiz F, Borrego J, González-Regalado ML, González NL, Carro B, Abad M (2008) Impact of millennial mining activities on sediments and microfauna of the Tinto River estuary (SW Spain). *Mar Pollut Bull* 56(7):1258–1264
- Ruiz F, Abad M, Bodergat AM, Carbonel P, Rodríguez-Lázaro J, González-Regalado ML, Toscano A, García EX, Prenda J (2013) Freshwater ostracods as environmental tracers. *Int J Environ Sci Technol* 10:1115–1128
- Rushdi AI, Rasul NM, Bazeyad A, Dumenden R (2019) Distribution and sources of hydrocarbon compounds in sediments from Obhur Lagoon: Red Sea coast of Saudi Arabia. *Oceanographic and Biological Aspects of the Red Sea*, pp 133–146
- Samir AM (2000) The response of benthic foraminifera and ostracods to various pollution sources: a study from two lagoons in Egypt. *J Foraminifer Res* 30(2):83–98
- Schönfeld J, Alve E, Geslin E, Jorissen F, Korsun S, Spezzaferri S (2012) The FOBIMO (FORaminiferal Bio-MONitoring) initiative—towards a standardized protocol for soft-bottom benthic foraminiferal monitoring studies. *Mar Micropaleontol* 94:1–13
- Scott HE, Aherne J, Metcalfe CD (2012) Fate and transport of polycyclic aromatic hydrocarbons in upland Irish headwater lake catchments. *The Scientific World Journal*, 2012
- Shamji VR, Vineesh TC (2017) Shallow-water tidal analysis at Sharm Obhur, Jeddah, Red Sea. *Arab J Geosci* 10:1–11
- Šmilauer P, Lepš J (2014) Multivariate analysis of ecological data using CANOCO. Cambridge University Press, New York, p 527
- Sundelin B, Elmgren R (1991) Meiofauna of an experimental soft bottom ecosystem—effects of macrofauna and cadmium exposure. *Mar Ecol Prog Ser* 70:245–255
- Tuuri EM, Leterme SC (2023) How plastic debris and associated chemicals impact the marine food web: a review. *Environ Pollut* :121156
- Van der Merwe C (2003) The assessment of the influence of treated underground mine water on the benthic fauna in a portion of the Blesbokspruit Ramsar Site. Mini thesis for Magister Artium in Environmental Management. Rand Afrikaans University, South Africa
- Walton WR (1952) Techniques for recognition of living foraminifera. *Scripps Institution of Oceanography*, p 125
- Wilson JJ, Al-Sofyani AA, Marimuthu N (2017) Current biodiversity and ecological status of scleractinian corals of Sharm Obhur, Jeddah, Saudi Arabian coast of the Red Sea. *Mar Biodivers* 47:1111–1121
- Yasuhara M, Yamazaki H, Irizuki T, Yoshikawa S (2003) Temporal changes of ostracode assemblages and anthropogenic pollution during the last 100 years, in sediment cores from Hiroshima Bay, Japan. *Holocene* 13(4):527–536
- Yasuhara M, Hunt G, Breitbart D, Tsujimoto A, Katsuki K (2012) Human induced marine ecological degradation: micropaleontological perspectives. *Ecol Evol* 2:3242–3268

Publisher's Note Springer Nature remains neutral with regard to jurisdictional claims in published maps and institutional affiliations.

Springer Nature or its licensor (e.g. a society or other partner) holds exclusive rights to this article under a publishing agreement with the author(s) or other rightsholder(s); author self-archiving of the accepted manuscript version of this article is solely governed by the terms of such publishing agreement and applicable law.



journals.

Dr. Mohammed H. Aljehdali is an associate professor of marine paleoenvironments specialized in marine microfossils and paleoecology of calcareous nannoplankton. His experience covers 15 years of participating in several scientific expeditions in the Atlantic and Pacific oceans. He also published over 40 articles in indexed



journal. **Ramadan M. El-Kahawy** is currently an assistant professor working for the Department of Geology, Faculty of Science, Cairo University, Egypt. He received his MSc (2016) and PhD (2021) from Cairo University. Dr. Ramadan M. El-Kahawy's research interests are focused on the environmental impact assessment using microorganisms, particularly benthic foraminifera and ostracods. Moreover, he focuses on the paleoecological implications and global warming during the Cretaceous, Paleogene, and Neogene periods in Egypt (Nile Delta, Gulf of Suez, and the Eastern and Western Desert provinces) and the Middle East using different microfossil groups (planktonic, benthic foraminifera, and calcareous nannofossils).



Mohamed Elhag obtained his Ph.D. degree from an Interdepartmental Program, School of Agricultural Sciences, University of Thessaly, Greece in Water Resources Management. Professor Elhag is currently a Tenured Track Professor of Remote Sensing at the Department of Water Resources, Faculty of Environmental Sciences, King Abdulaziz University, Saudi Arabia. Professor Elhag is a Research Fellow at the State Key Laboratory, of Remote Sensing, Aerospace Information Research Institute, Chinese Academy of Science, Beijing 100101, China. Research Fellow at the Department of Geoinformation in Environmental Management, CI-HEAM/Mediterranean Agronomic Institute of Chania, Chania 73100, Greece. Visiting Professor at the Department of Applied Geosciences, Faculty of Science, German University of Technology, Oman. He is the author of several articles published in reputed journals and is a member of different international working groups related to his background. Prof. Elhag teaches a wide variety of Remote Sensing courses for under and postgraduate students.



Bandar Al-Mur is an Associate Professor in Environmental Sciences and a faculty member in the Environmental Sciences Department at King Abdulaziz University. He earned his Ph.D. in Environmental Engineering from Southern Methodist University (SMU), USA, in 2017. His research interests include environmental monitoring of chemical pollutants in water and sediments, the fate and effects of inorganic and organic compounds in marine environments, and the remediation of toxic heavy metals and hydrocarbons from contaminated sites.



Andrew N. Quicksall is an Associate Professor at the Civil and Environmental Engineering Department, Lyle School of Engineering Southern Methodist University, USA. He got his MSc. From Washington State University – Pullman, WA in 2000, and PhD from Dartmouth College – Hanover, NH in 2009. My research interests are focused on Water Chemistry, heavy metals, and Soil Chemistry.



Faisal Alsaq is an assistant professor in the Hydrographic Department, Faculty of Maritime Studies, King Abdulaziz University, Saudi Arabia. I received my M. Eng. from the Department of Geodesy and Geomatics Engineering with Ocean Mappin Group, University of New Brunswick, Canada. In 2017, I received my PhD in Geospatial Science from Curtin University in Australia. I have more than 20 years of extensive experience in leadership and project management. Currently, I am the general supervisor of the Marine Vessel Center at the university. I worked on managing many marine projects in the Red Sea and the Arabian Gulf. In addition, I led my own business and established a company responsible for marine surveys in the Middle East.



Ibrahim Mohamed Ghandour an Egyptian Professor of sedimentology and sequence stratigraphy, working at the Marine Geology Department, Faculty of Marine Sciences, King Abdulaziz University, Saudi Arabia. Additionally, I have a permanent position at the Geology Department, Faculty of Science, Tanta University, Egypt. I have research interests in marine sediments; chemical and mineralogical composition, geoenvironmental assessment, siliciclastic facies analysis, impact of climate and sea-level changes on coastal sediments, and paleoenvironmental interpretations.